

MANUSCRIPT

Significantly enhanced photocatalytic degradation of Methylene Blue using rGO-SnO₂ nanocomposite under natural sunlight and UV light irradiation

M. Bakhtiar Azim^{a,e*}, Muhammad Hasanuzzaman^b, Md. Shakhawat Hossain Firoz^c, Md. Abdul Gafur^d, A.S.W Kurny^a, Fahmida Gulshan^{a*}

^aDepartment of Materials and Metallurgical Engineering, Faculty of Engineering, Bangladesh University of Engineering and Technology, Dhaka-1000, Bangladesh.

^aProfessor [retired], Department of Materials and Metallurgical Engineering, Faculty of Engineering, Bangladesh University of Engineering and Technology, Dhaka-1000, Bangladesh.

^aProfessor, Department of Materials and Metallurgical Engineering, Faculty of Engineering, Bangladesh University of Engineering and Technology, Dhaka-1000, Bangladesh.

^bAssistant Professor, Department of Glass and Ceramics Engineering, Faculty of Engineering, Bangladesh University of Engineering and Technology, Dhaka-1000, Bangladesh.

^cAssociate Professor, Department of Chemistry, Faculty of Engineering, Bangladesh University of Engineering and Technology, Dhaka-1000, Bangladesh.

^dPilot Plant and Process Development Center, Bangladesh Council of Scientific and Industrial Research (PP and PDC, BCSIR), Dhaka-1205, Bangladesh.

^eSchool of Engineering Science, Faculty of Applied Science, Simon Fraser University, Burnaby, British Columbia, Canada.

Dr. Fahmida Gulshan, E-mail: fahmidagulshan@mme.buet.ac.bd

M. Bakhtiar Azim, E-mail: bakhtiar31.mme@gmail.com; mbazim@sfu.ca

ABSTRACT

Environmental contamination and human exposure to dyes have dramatically increased over the past decades because of their increasing use in such industries as textiles, paper, plastics, tannery and paints. These dyes can cause deterioration in water quality by imparting color to the water and inducing the photosynthetic activity of aquatic organisms by hindering light penetration. Moreover, some of the dyes are considered carcinogenic and mutagenic for human health. Therefore, efficient treatment and removal of dyes from wastewater have attracted considerable attention in recent years. Photocatalysis, due to its mild reaction condition, high degradation, broad applied area and facile manipulation, is a promising method of solving environmental pollution problems. In this paper, we report the synthesis of reduced Graphene Oxide-Tin Oxide (rGO-SnO₂) nanocomposite and the effectiveness of this composite in decolorizing and degrading Methylene Blue (MB). Tin Oxide was prepared by liquid phase co-precipitation method and reduced Graphene Oxide-Tin Oxide (rGO-SnO₂) nanocomposite was prepared by solution mixing method. Tin Oxide (SnO₂) nanoparticles (NPs) have been ardently investigated as photocatalyst for water purification and environment decontamination but the photon generated electron and hole pair (EHP) recombination is one of the limiting factors. Reduced Graphene Oxide-Tin Oxide (rGO-SnO₂) nanocomposite is very efficient to overcome this limitation for photocatalytic application. The as-synthesized GO, SnO₂, GO-SnO₂, rGO and rGO-SnO₂ nanocomposite were characterized by X-ray Diffraction (XRD), Scanning Electron Microscopy (SEM), Energy Dispersive X-ray spectroscopy (EDX) and Fourier Transform Infrared spectroscopy (FTIR). The XRD data confirms the sharp peak at $2\theta=10.44^\circ$ corresponding to (002) reflection of GO with interlayer d-spacing of 8.46 \AA indication of successful preparation of GO by oxidation of graphite. Moreover,

the diffraction peak shifts from $2\theta=10.44^\circ$ to $2\theta=23.31^\circ$ confirm successful synthesis of rGO as well. SEM image shows the morphology of GO, SnO₂, GO-SnO₂ and rGO-SnO₂. EDX studies are carried out to investigate the elemental composition and purity of the sample by giving all the elements present in the GO, SnO₂, GO-SnO₂ and rGO-SnO₂. The presence of functional groups was identified by FTIR. The rGO-SnO₂ (1:10) nanocomposite shows an efficient photodegradation efficiency of ~94% and ~95% under natural sunlight and UV light irradiation respectively for Methylene Blue (MB) within 15 minutes. Furthermore, the degradation kinetics of MB is also studied in this paper as well.

Keywords: reduced Graphene Oxide, Tin Oxide, Kinetics, Photodegradation, Methylene Blue.

1. INTRODUCTION

With the rapid development of textile industry in recent years, more and more new types of dyes, such as Methylene Blue, have been produced. According to World Bank report, almost 20% of global industrial water pollution comes from the dyeing and finishing processes of textiles [1]. The discharge of azo dyes, which are stable and carcinogenic, into water bodies are harmful to human health, and cause such illness as cholera, diarrhea, hypertension, precordial pain, dizziness, fever, nausea, vomiting, abdominal pain, bladder irritation, staining of skin etc. [2]. Dyes also affect aquatic life by hindering the photosynthesis process of aquatic plants, eutrophication, and perturbation [3,4]. Numerous techniques, such as activated carbon adsorption (physical method), chlorination (chemical method), and aerobic biodegradation (biochemical method) [4] have been applied to treat textile wastewater. However, further treatments are needed, which create such secondary pollution in the environment, as the breakdown of parent cationic dyes to Benzene, NO₂, CO₂ and SO₂ [6]. Advanced oxidation

processes (AOPs) are widely applied to mineralize dyes into CO₂ and H₂O [7, 8]. AOPs include ozonation, photolysis, and photocatalysis with the aid of oxidants, light, and semiconductors. Photocatalytic degradation is initiated when the photocatalysts absorb photons (UV) to generate electron-hole pairs on the catalyst surface. The positive hole in the valence band (h_{VB}^+) will react with water to form hydroxyl radical ($\bullet\text{OH}$), followed by the oxidization of pollutants to CO₂ and H₂O [9].

Methylene Blue (MB), also known as Basic Blue 9, is a cationic azo dye (Table 1). MB is widely used in textile industries for dye processing, and upto 50% of the dyes consumed in textile industries are azo dyes [9-11]. In the past few years, several catalysts such as TiO₂ [6], BiFeO₃ [5], ZnS [13] and ZnO [9] have been used to degrade MB and the results are summarized in (Table 2).

[Insert Table 1 and Table 2]

Carbon based materials combined with metal oxides are known to have improved photocatalytic activity. Graphene, a two-dimensional material having sp² bonded carbon atoms arranged in a honeycomb lattice with a one-atom-thick, has recently attracted a great deal of scientific attention among the researchers. Owing to its extraordinary advantages, such as large theoretical specific surface area (2630 m²/g), superior electronic and excellent chemical stability, therefore graphene is considered as an outstanding support for photocatalytic application. It was first isolated from 3D graphite by mechanical exfoliation. It has also been reported that the graphene-metal oxide composite possess good photocatalytic activity, compared to the pure metal oxide.

Numerous chemical, thermal, microwave and microbial/bacterial methods have been used in the synthesis of rGO [15]. Chemical exfoliation is preferable due to its large-scale production and low cost. Chemical exfoliation involves four steps, oxidation of graphite powder, dispersion of graphite oxide (GTO) to graphene oxide (GO), GTO exfoliation by ultrasonication to produce graphene oxide (GO) and finally, reduction of GO to rGO using a reducing agent [16]. Reduced Graphene oxide (rGO) has less oxygen functional groups than graphene oxide (GO). rGO has a surface area of 833 m²/g compared to 736.6 m²/g and 400 m²/g for GO and graphite [30-31]. rGO, with its unique electronic properties, large surface area and high transparency, contributes to facile charge separation and adsorptivity in its structure. As a potential photocatalytic material, rGO-SnO₂ has been used in the decolorization of Methylene Blue [20] and Rhodamine B [20].

SnO₂ is a capable candidate to photocatalyze and complete oxidative mineralization of MB. Chemical contamination of water streams has become crucial issue of human life. Wastewater treatment plays an important role in reducing the toxic elements in wastewater. Heterogeneous photocatalysis can be applied to remove contaminants existing in wastewater effluent. Heterogeneous photocatalysis includes such reactions as organic synthesis, water splitting, photo-reduction, hydrogen transfer and metal deposition, disinfection, water treatment, removal of gaseous pollutants etc. It has become an increasingly viable technology in environmental decontamination. Photocatalytic oxidation of such organic compounds are derived by semiconductor materials like TiO₂, ZnO, CdS and CuO. These are now-a-days widely used in the environment as photocatalysts. They have band-gap of 3.6 eV, when other photocatalysts have higher band-gap. They are used extensively due to their low-cost, non-

toxicity, high activity, large chemical stability, very low aqueous solubility and environmental friendly characteristics. Tin-assisted photocatalytic oxidation is an alternative method for purification of air and water streams. Also, in water splitting, the driving force for electrons is provided by energy of light. When SnO₂ is exposed to light, photocatalytic reaction is initiated. rGO-SnO₂ nanocomposite is very promising to overcome the limitation for photocatalytic application. rGO with its large surface area, unique electronic properties and high transparency, contributes to spatial charge separation and adsorptivity in this hybrid structure.

In this investigation, we report a facile method to prepare rGO-SnO₂ nanocomposite. It was synthesized via solution mixing method. The photocatalytic performances of the prepared GO, SnO₂, GO-SnO₂, rGO and rGO-SnO₂ nanomaterials were evaluated in the degradation of Methylene Blue (MB) under natural sunlight and UV light irradiation.

2. EXPERIMENTAL SECTION

2.1. Chemicals and Materials

Graphite fine powder (~325 mesh) was purchased from Alfa Aesar. Sodium Nitrate, Tin (II) Chloride Di-hydrate (98%), Potassium permanganate (99%), Hydrochloric acid (37%), Hydrogen Peroxide (30%), Silver Nitrate (99.8%), Ammonia solution (25%), Urea and Hydrazine Hydrate (99%) were purchased from Sigma-Aldrich (Steinheim, Germany). Sulfuric acid (98%) was obtained from Merck (Darmstadt, Germany). The chemicals were used without further purifications. Methylene Blue (MB) powder from Merck (Darmstadt, Germany) was used as the

model organic dye in this study. Deionized water (DI water) was used throughout the experiments.

2.2. Synthesis of GO

Graphene oxide was produced through the modified Hummers' method [35] by oxidizing the graphite powder. In a typical synthesis, 5 gm of graphite powder and 2.5 gm NaNO_3 were mixed with 115 ml H_2SO_4 (conc. 98%). 15 gm of KMnO_4 was slowly added and stirred in an ice-bath for 1 h below 20°C . The mixture was heated to 35°C and was constantly stirred for 2 hours. The beaker was placed on an oil bath, heated to and maintained at a temperature $95^\circ\text{C}\sim 98^\circ\text{C}$, for 15 minutes. 250 ml DI water was added slowly under constant stirring. The mixture was cooled to room temperature. The beaker was then placed on the oil bath for additional 60 minutes at a constant temperature 60°C . 150 ml DI water was added under constant stirring. Finally, 50 ml (30%) H_2O_2 was added in drops and stirred for 2 hours. Washing, filtration and centrifugation (6000 rpm) were done until the removal of Cl^- ions by using DI water. Finally, the resulting precipitate was dried at 70°C for 24 hours in an oven giving thin sheets which was Graphite Oxide (GTO). Graphite Oxide was made into fine powder form by grinding and then GTO powder was finely dispersed in DI Water. At last, ultrasonication was done for the complete exfoliation of GTO to GO.

2.3. Synthesis of SnO_2

SnO_2 was produced through the liquid phase co-precipitation method. 2 gm Stannous Chloride Di-hydrate ($\text{SnCl}_2 \cdot 2\text{H}_2\text{O}$) was dissolved in 100 ml DI Water. After complete dissolution, ammonia solution (25%) was added in drops to the above solution under stirring. The resulting gel type

precipitate was filtered and dried at 80°C for 24 hours to remove water molecules. Finally, tin oxide nanopowders were formed through calcination at 550°C for 4-6 hours.

2.4. Synthesis of GO-SnO₂

GO-SnO₂ was prepared through the solution mixing method. At first, 2.6 gm SnCl₂.2H₂O was added to HCl (37%) and stirred for 1 hour. Then, 260 mg GO was dispersed in 200 ml DI water by using ultrasonication for 45 minutes. Both solutions were mixed and stirred rigorously for 15 minutes. Again ultrasonication was done for 15 minutes. After that, washing, filtration and centrifugation were done with DI water till a neutral pH was obtained. The sediment was collected and dried at 80°C for 24 hours. Finally, thin sheet of GO-SnO₂ nanocomposite was collected and grinded into GO-SnO₂ nano powder.

2.5. Synthesis of rGO

260 mg GO was dispersed in DI water and then exfoliated by ultrasonication for 1 hour. Subsequently, 5 ml of 99% Hydrazine Hydrate was added and the solution was heated in heating mantle with stirrer at 100°C under a water cooled condenser for 24 hours. After heating at 100°C, the solution turns from brown to black precipitate. The product was cooled, filtered and washed with DI water for 4 times. Finally, the product was dried overnight at 60°C.

2.6. Synthesis of rGO-SnO₂

rGO-SnO₂ was prepared also through the solution mixing method. At first, 2.6 gm SnCl₂.2H₂O was added to HCl (37%) and diluted with DI water to give SnCl₂-HCl solution. Then, 260 mg GO was dispersed in DI water by using ultrasonication for 30 minutes to form a colloidal suspension. The GO solution was added to a SnCl₂-HCl solution and ultrasonication was done for 15 minutes. 2.6 gm Urea was then added to the resulting solution and stirred for 15 minutes. The solution was

heated to 95°C for 6 hours. The precipitate obtained was separated by centrifugation (6000 rpm) and subsequent washing to remove excess Cl⁻ ions. The resulting product was dried in an oven at 110°C for 6 hours.

3. CHARACTERIZATION

The X-ray diffraction pattern of GO, SnO₂, GO-SnO₂, rGO and rGO-SnO₂ was recorded by a Bruker, D8 Advance diffractometer (Germany). The sample was scanned from 5° to 80° using Cu K α radiation source ($\lambda = 1.5406 \text{ \AA}$) at 40 kV and 30 mA with a scanning speed of 0.01°s⁻¹. The surface morphology of GO, SnO₂, GO-SnO₂ and rGO-SnO₂ was observed by FESEM-JEOL (FEG-XL 30S) Field Emission Scanning Electron microscope (FESEM). FTIR spectra of GO, SnO₂, and rGO-SnO₂ was recorded by Agilent Cary 670 FTIR spectrometer. The photodegradation percentage of MB was determined by using an ultraviolet-visible spectrophotometer (Shimadzu-UV-1601) at $\lambda_{\text{max}} = 664$ nm and wavelength region between 400 and 800 nm. DI water was used as a reference material.

4. PHOTOCATALYTIC REACTION

Photocatalytic experiments were carried out by photodegrading MB using Shimadzu-UV-1601 UV-Vis spectroscopy. The solution of MB (pH~7) without rGO-SnO₂ was left in a dark place for 24 hrs. Then, the dye solution was exposed to natural sunlight irradiation and UV irradiation and there was no decrease in the concentration of dye. In a typical experiment, 7.5 mg of rGO-SnO₂ was added into a 50 mL 0.05 mM MB solution. Before illumination, the suspensions were continuously shaken and kept in dark for 60 min to reach an adsorption-desorption equilibrium between the photocatalyst and dye solution. The suspensions were then exposed to natural sunlight and UV irradiation. Samples were taken from irradiation at regular time intervals (0 min,

10 min, 15 min, 30 min, 45 min and 60 min for MB) filtered out to remove the rGO-SnO₂. Irradiation was carried out in falcon tubes. The same procedure was repeated for both GO, SnO₂, rGO and GO-SnO₂. The initial pH of solution (pH~7) was adjusted by small amount of 0.1 M NaOH and 0.1 M HCl when required.

Photodegradation was also observed for 0.05 mM 50 ml MB solution using only GO, SnO₂, GO-SnO₂ and rGO. The photodegradation efficiency of MB was determined by using the equation shown below:

$$\text{Photodegradation efficiency (\%)} = [(C_0 - C_t) / C_0] \times 100\% = [(A_0 - A_t) / A_0] \times 100\% \text{ -----(1)}$$

[According to 'Beer-Lambert Law']

Where, C₀ is the initial concentration of MB, C_t is the concentration of MB at time, t and A₀ is the initial absorbance of MB, A_t is the absorbance of at time, t.

5. RESULTS AND DISCUSSION

5.1. Characterization of Photocatalysts

XRD

The powder X-ray diffraction pattern of GO shows a broadened diffraction peak (Fig. 1) at around 2θ=10.44°, which corresponds to the (002) reflection of stacked GO sheets with interlayer d-spacing of 8.46°. rGO shows diffraction peak at around 2θ=23.31° with interlayer d-spacing of 7.62 Å. XRD patterns of SnO₂ nanoparticles (Fig. 1) shows the diffraction peaks of (110), (101),

(111) and (211) at 2θ of 26.8° , 33.9° , 37.9° and 51.8° respectively which matches well with JCPDS card # 41-1445. The average crystallite size can be determined using “Scherrer Formula”:

$$B = (k\lambda)/(\beta \cos\theta_\beta) \text{-----(2)}$$

Where, B is the average crystallite size (nm), k is the factor of 0.9, λ is the wavelength of radiation source used is 1.5406 \AA , β is the full width of half maximum peak (FWHM), θ_β is the angle at maximum peak. The average crystallite size of SnO_2 is $\sim 35 \text{ nm}$ (eq. 2). The XRD pattern of rGO- SnO_2 nanocomposite (Fig. 1) shows SnO_2 peaks but the intensity of the peaks are reduced and broaden when compared with XRD pattern of individual rGO and SnO_2 .

[Insert Fig. 1]

SEM and EDX

SEM images of rGO- SnO_2 structure are shown in ((Fig. 2(e)). The average particle size of SnO_2 is $\sim 46 \text{ nm}$ using ImageJ analysis ((Fig. 2(b)). SEM images of rGO- SnO_2 shows presence of SnO_2 nanoparticles in the rGO layer by layer sheets.

[Insert Fig. 2]

EDX results indicating successful incorporation of oxygen by modified Hummers method in graphite layers and formation of oxygen based functional groups in GO with ratio of $C/O=4.58$ ((Fig. 3(a)). It also shows successful synthesis of SnO_2 nanoparticles ((Fig. 3(b)). It gives clear indication of incorporation of SnO_2 nanoparticles in rGO layer by layer sheets ((Fig. 3(d)).

[Insert Fig. 3]

FTIR

The FTIR spectra of GO, SnO₂ and rGO-SnO₂ was recorded by Agilent Cary 670 FTIR spectrometer. FTIR analysis of GO shows broad absorption spectrum observed at ~3420 cm⁻¹ corresponding O-H stretching vibration indicating existence of absorbed water molecules and structural O-H groups in GO. The broad peak appeared in GO spectrum depicted the presence of O-H and C-H stretching. Besides, a band at 1747 cm⁻¹ might be related to not only the C=O stretching motion of -COOH groups situated at the edges and defects of GO lamellae but also that of ketone or quinone groups. The peak near 1700-1550 cm⁻¹ widens and moves to 1565 cm⁻¹ that reflects the presence of un-oxidized aromatic regions. The FTIR spectrum of Tin Oxide shows broad not sharp absorption band ~3420 cm⁻¹ corresponding O-H stretching vibration due to absorbed water molecules. A band at ~612 cm⁻¹ related to O-Sn-O stretching. Broad and sharp absorption spectrum observed at ~3420 cm⁻¹ corresponding O-H stretching vibration in rGO-SnO₂. Peak at 1625cm⁻¹ corresponding O-H bending vibration indicating existence of absorbed water molecules and structural O-H groups in rGO-SnO₂ by FTIR. Similarly, a sharp band at ~612 cm⁻¹ related to O-Sn-O stretching in rGO-SnO₂ refers to the incorporation of SnO₂ particles. (Fig. 4)

[Insert Fig. 4]

5.2. Photocatalytic Activity

5.2.1. Conditions and Parameters for Photocatalytic Activity Measurement

The concentration and amount of the dye used for the experiment were 0.05 mM and 50 ml respectively. Weight of the samples used for the experiment was 7.5 mg each. For the experiment

pH was considered as ~7 and temperature outside was 29 °C - 33° C. The most crucial parameters of the experiment were (i) Natural Sunlight Irradiation, (ii) UV light Irradiation, (iii) Irradiation Time Effect and (iv) Catalyst Types.

5.2.2. Photocatalytic Activity Evaluation

UV-Vis Spectroscopy was used to measure absorbance of the dye solution at regular time intervals using rGO-SnO₂. Controlled experiments were also carried out to confirm that the degradation of MB by UV-Vis for visible range. Experiments were repeated for other photocatalysts also.

$$\text{Photodegradation Efficiency (\%)} = [(C_0 - C_t) / C_0] \times 100\% = [(A_0 - A_t) / A_0] \times 100\% \text{-----(3)}$$

Here, C₀= Concentration of MB at '0' min, C_t= Concentration of MB at 't' min, A₀= Absorbance of MB at '0' min, A_t= Absorbance of MB at 't' min

Time-dependent absorption spectra of MB solution shows enhanced photocatalytic activity of rGO-SnO₂ compared to SnO₂ and rGO under natural sunlight and UV irradiation (Fig. 5 and Fig 7).

[Insert Fig. 5 and Fig. 6]

[Insert Fig. 7 and Fig. 8]

It is clearly seen from the ((Fig. 6(a) and Fig. 8(a)) that rGO-SnO₂ having lesser absorbance compared to GO, SnO₂, GO-SnO₂ and rGO. From ((Fig. 6(b) and Fig. 8(b)) with irradiation time concentration of MB solution reduces significantly by using rGO-SnO₂ nanocomposite with

respect to others under natural sunlight and UV light irradiation. Under natural sunlight and UV light irradiation rGO-SnO₂ nanocomposite showed ~94% and ~95% photodegradation efficiency respectively within 15 minutes compared to other photocatalysts ((Fig. 9(a) and Fig. 9(b)). The most outstanding factor of this experiment is under UV light irradiation the degradation efficiency of GO-SnO₂ has increased remarkably from ~61% to 94% after 30 minutes ((Fig. 9(a) and Fig. 9(b)).

[Insert Fig. 9]

6. ADSORPTION KINETICS

6.1. Pseudo First Order

The MB photo degradation was fitted to pseudo-first order kinetics by referring to the Langmuir-Hinshelwood kinetic model :

$$\ln\left(\frac{C_0}{C_t}\right) = k_1 t \text{-----(4)}$$

Where, C_t = Concentration of MB at time, t, C₀ = Initial concentration of MB, k₁ = Pseudo-first order rate constant.

The k₁ values of respective concentrations was determined from knowing the values C_t and was listed in Table 3.

6.2. Pseudo Second Order

Pseudo second-order equilibrium adsorption equation can be expressed as follows:

$$\frac{1}{C_t} = \frac{1}{C_0} + 2k_2 t \text{-----(5)}$$

Where, C_t = Concentration of MB at time t , C_0 = Initial concentration of MB, k_2 = Pseudo-second order rate constant.

The k_2 values of respective concentrations was determined from knowing the values C_t and was listed in Table 4.

6.3. Adsorption Kinetics Evaluation

The correlation coefficient (R^2) values are close to 1 observed in Table 3 than Table 4. Therefore, it gives clear indication that rGO-SnO₂ obeys the pseudo-first order kinetic model under natural sunlight irradiation.

[Insert Table 3 and Table 4]

[Insert Fig. 10]

The correlation coefficient (R^2) values are close to 1 observed in Table 5 than Table 6. Therefore, it gives clear indication that rGO-SnO₂ obeys the pseudo-first order kinetic model under UV light irradiation.

[Insert Table 5 and Table 6]

[Insert Fig. 11]

7. CONCLUSIONS

Results of characterization showed that GO, SnO₂, GO-SnO₂, rGO and rGO-SnO₂ were synthesized successfully. Degradation of 0.05 mM 50 ml Methylene Blue under direct sunlight and UV light

irradiation with 7.5 mg rGO-SnO₂ nanocomposite as a photocatalyst takes around 15 min for ~94% and ~95% degradation respectively compared to other catalysts. The most significant result of this experiment is under UV light degradation efficiency of GO-SnO₂ enhanced remarkably compared to other photocatalysts within 30 minutes (from ~61% to ~94%). Wide band gap of SnO₂ is tuned using rGO therefore it shows enhanced photocatalytic performance compared to SnO₂ only. Moreover, the degradation kinetics is also studied and rGO-SnO₂ maintains the pseudo-first order kinetic model.

CONFLICTS OF INTERESTS

There are no conflicts to declare.

ACKNOWLEDGEMENTS

This work was supported by Department of Materials and Metallurgical Engineering (MME, BUET), The Pilot Plant and Process Development Center, Bangladesh Council of Scientific and Industrial Research (PP and PDC, BCSIR), Department of Glass and Ceramics Engineering (GCE, BUET) and Department of Chemistry, BUET.

REFERENCES:

1. APHA, 2005. Standard methods for the examination of water and waste water, 21 ed. American Water Works Association and Water Environment Federation.
2. Lee, K.M.; Abdul Hamid, S.B.; Lai, C.W. "Multivariate analysis of photocatalytic-mineralization of Eriochrome Black T dye using ZnO catalyst and UV irradiation," Mater. Sci. Semicond. Process. 2015, 39, 40–48.

3. Mehra, M.; Sharma, T.R. "Photocatalytic degradation of two commercial dyes in aqueous phase using photocatalyst TiO₂," *Adv. Appl. Sci. Res.* 2012, 3, 849–853.
4. Vinothkannan, M.; Karthikeyan, C.; Gnana kumar, G.; Kim, A.R.; Yoo, D.J. "One-pot green synthesis of reduced graphene oxide (RGO)/Fe₃O₄ nanocomposites and its catalytic activity toward methylene blue dye degradation," *Spectrochim. Acta A Mol. Biomol. Spectrosc.* 2015, 136, 256–264.
5. Soltani, T.; Entezari, M.H. "Photolysis and photocatalysis of methylene blue by ferrite bismuth nanoparticles under sunlight irradiation," *J. Mole. Cat.* 2013, 377, 197-203.
6. Dariani, R.S.; Esmaili, A.; Mortezaali, A.; Dehghanpour, S. "Photocatalytic reaction and degradation of methylene blue on TiO₂ nano-sized particles," *Optik.* 2016, 127, 7143-7154.
7. Chan, S.H.S.; Wu, Y.T.; Juan, J.C.; Teh, C.Y. "Recent developments of metal oxide semiconductors as photocatalysts in advanced oxidation processes (AOPs) for treatment of dye waste-water," *J. Chem. Technol. Biotechnol.* 2011, 86, 1130–1158.
8. Zhang, W.; Naidu, B.S.; Ou, J.Z.; O'Mullane, A.P.; Chrimes, A.F.; Carey, B.J.; Wang, Y.; Tang, S.Y.; Sivan, V.; Mitchell, A.; et al. "Liquid metal/metal oxide frameworks with incorporated Ga₂O₃ for photocatalysis," *ACS Appl. Mater. Interfaces* 2015, 7, 1943–1948.
9. Kansal, S.; Kaur, N.; Singh, S. "Photocatalytic degradation of two commercial reactive dyes in aqueous phase using nanophotocatalysts," *Nanoscale Res. Lett.*, 2009, 4, 709–716.
10. Ong, W.J.; Yeong, J.J.; Tan, L.L.; Goh, B.T.; Yong, S.T.; Chai, S.P. "Synergistic effect of graphene as a co-catalyst for enhanced daylight-induced photocatalytic activity of Zn_{0.5}Cd_{0.5}S synthesized

via an improved one-pot co-precipitation-hydrothermal strategy,” *R. Soc. Chem. Adv.*, 2014, 4, 59676–59685.

11. Sahel, K.; Perol, N.; Chermette, H.; Bordes, C.; Derriche, Z.; Guillard, C. “Photocatalytic decolourization of remazol black 5 (RB5) and procion red MX-5B-Isotherm of adsorption, kinetic of decolourization and mineralization,” *Appl. Catal. B Environ.*, 2007, 77, 100–109.

12. Lucas, M.S.; Tavares, P.B.; Peres, J.A.; Faria, J.L.; Rocha, M.; Pereira, C.; Freire, C. “Photocatalytic degradation of reactive black 5 with TiO₂-coated magnetic nanoparticles,” *Catal. Today*, 2013, 209, 116–121.

13. Goharshadi, E.K.; Hadadian, M.; Karimi, M.; Azizi-Toupkanloo, H. “Photocatalytic degradation of reactive black 5 azo dye by zinc sulfide quantum dots prepared by a sonochemical method,” *Mater. Sci. Semicond. Process.*, 2013, 16, 1109–1116.

14. Laohaprapanon, S.; Matahum, J.; Tayo, L.; You, S.J. “Photodegradation of reactive black 5 in a ZnO/UV slurry membrane reactor,” *J. Taiwan Inst. Chem. Eng.*, 2015, 49, 136–141.

15. Bianco, A.; Cheng, H.M.; Enoki, T.; Gogotsi, Y.; Hurt, R.H.; Koratkar, N.; Kyotani, T.; Monthieux, M.; Park, C.R.; Tascon, J.M.D.; et al. “All in the graphene family-A recommended nomenclature for two-dimensional carbon materials,” *Carbon*, 2013, 65, 1–6.

16. Cao, N.; Zhang, Y. “Study of reduced graphene oxide preparation by Hummers’ method and related characterization,” *J. Nanomater.*, 2015.

17. Singh, V.; Joung, D.; Zhai, L.; Das, S.; Khondaker, S.I.; Seal, S. “Graphene based materials: Past, present and future,” *Prog. Mater. Sci.*, 2011, 56, 1178–1271.

18. Wang, D.T.; Li, X.; Chen, J.F.; Tao, X. "Enhanced photoelectrocatalytic activity of reduced graphene oxide/TiO₂ composite films for dye degradation," *Chem. Eng. J.* 2012, 198, 547–554.
19. Dong, S.Y.; Cui, Y.R.; Wang, Y.F.; Li, Y.K.; Hu, L.M.; Sun, J.Y.; Sun, J.H. "Designing three-dimensional acicular sheaf shaped BiVO₄/reduced graphene oxide composites for efficient sunlight-driven photocatalytic degradation of dye wastewater," *Chem. Eng. J.*, 2014, 249, 102–110.
20. Liu, X.J.; Pan, L.K.; Lv, T.; Sun, Z.; Sun, C.Q. "Visible light photocatalytic degradation of dyes by bismuth oxide-reduced graphene oxide composites prepared via microwaved-assisted method," *J. Colloid Interface Sci.* 2013, 408, 145–150.
21. Yao, Y.J.; Xu, C.; Miao, S.D.; Sun, H.Q.; Wang, S.B. "One-pot hydrothermal synthesis of Co(OH)₂ nanoflakes on graphene sheets and their fast catalytic oxidation of phenol in liquid phase," *J. Colloid Interface Sci.*, 2013, 40, 230–236.
22. Bose, S.; Kuila, T.; Uddin, M.E.; Kim, N.H.; Lau, A.K.T.; Lee, J.H. "In-situ synthesis and characterization of electrically conductive polypyrrole/graphene nanocomposites," *Polymer*, 2010, 51, 5921–5928.
23. Krishnamoorthy, K.; Kim, G.S.; Kim, S.J. "Graphene nanosheets: Ultrasound assisted synthesis and characterization," *Ultrason. Sonochem.*, 2013, 20, 644–649.
24. Satheesh, K.; Jayavel, R. "Synthesis and electrochemical properties of reduced graphene oxide via chemical reduction using thiourea as a reducing agent," *Mater. Lett.*, 2013, 113, 5–8.

25. Zainy, M.; Huang, N.M.; Kumar, S.V.; Lim, H.N.; Chia, C.H.; Harrison, L. "Simple and scalable preparation of reduced graphene oxide-silver nanocomposites via rapid thermal treatment," *Mater. Lett.*, 2012, 89, 180–183.
26. Stankovich, S.; Dikin, D.A.; Piner, R.D.; Kohlhaas, K.A.; Alfred, K.; Jia, Y.Y.; Wu, Y.; Nguyen, S.T.; Ruoff, R.S. "Synthesis of graphene-based nanosheets via chemical reduction of exfoliated graphite oxide," *Carbon*, 2007, 45, 1558–565.
27. Apollo, S.; Moyo, S.; Mabuo, G.; Aoyi, O. "Solar photodegradation of methyl orange and phenol using silica supported ZnO catalyst," *Int. J. Innov. Manag. Technol.*, 2014, 5, 203–206.
28. Ong, S.A.; Min, O.M.; Ho, L.N.; Wong, Y.S. "Comparative study on photocatalytic degradation of Mono Azo Dye Acid Orange 7 and Methyl Orange under solar light irradiation," *Water Air Soil Pollut.*, 2012, 223, 5483–5493.
29. Kumar, K.V.; Porkodi, K.; Rocha, F. "Langmuir-Hinshelwood Kinetics-A theoretical study," *Catal. Commun.*, 2008, 9, 82–84.
30. Mohabansi, N.P.; Patil, V.B.; Yenkie, N. "A comparative study on photo degradation of methylene blue dye effluent by advanced oxidation process by using TiO₂/ZnO photo catalyst," *Rasayan J. Chem.*, 2011, 04, 814-819.
31. Navajas, P.M.; Asenjo, N.G.; Santamaria, R.; Menendez, R.; Corma, A.; Garcia, H. "Surface Area Measurement of Graphene Oxide in Aqueous Solutions," *Langmuir*, 2013, 29, 13443–13448.
32. Reza, K.M.; Kurny, A.S.W; Gulshan, F. "Photocatalytic Degradation of Methylene Blue by Magnetite + H₂O₂ + UV Process," *Int. J. Env. Scn. Dev.*, 2016, 7 (5), 325-329.

33. M. Bakhtiar Azim, Intaqer Arafat Tanim, Riad Morshed Rezaul, Rizwan Tareq, Arafat Hossain Rahul, A.S.W Kurny, Fahmida Gulshan, “Degradation of Methylene Blue using Graphene Oxide-Tin Oxide Nanocomposite as Photocatalyst”, Proceedings of the 1st International Conference on Engineering Materials and Metallurgical Engineering, Paper ID: C117, 202-209, 22- 24 December, 2016, Bangladesh Council of Scientific and Industrial Research (BCSIR) Dhaka, Bangladesh.

34. M. Bakhtiar Azim, Intaqer Arafat Tanim, Riad Morshed Rezaul, M. Mozammal Hosen, Fahmida Gulshan , A.S.W Kurny, “Graphene-Oxide for Efficient Photocatalytic Degradation of Methylene Blue under Sunlight and Its Kinetic Study”, International Conference on Computer, Communication, Chemical, Materials and Electronic Engineering (IC⁴ME²), Paper ID: 12, 38-43, 26-27 January, 2017.

FIGURES

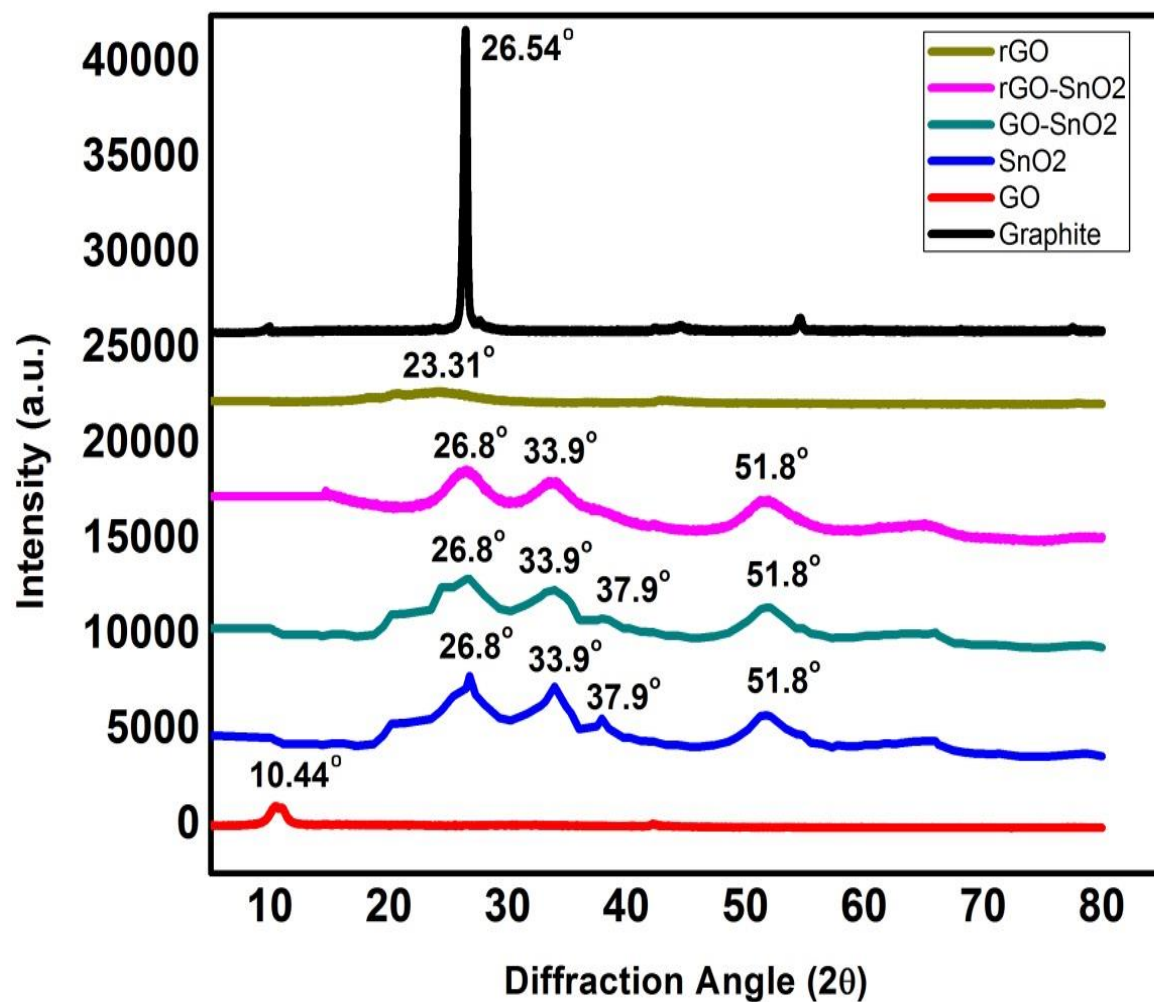
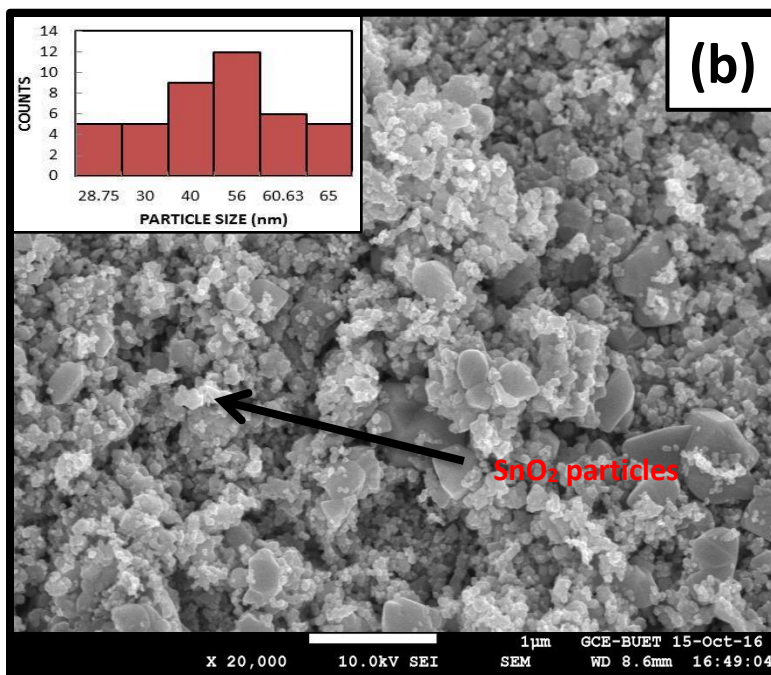
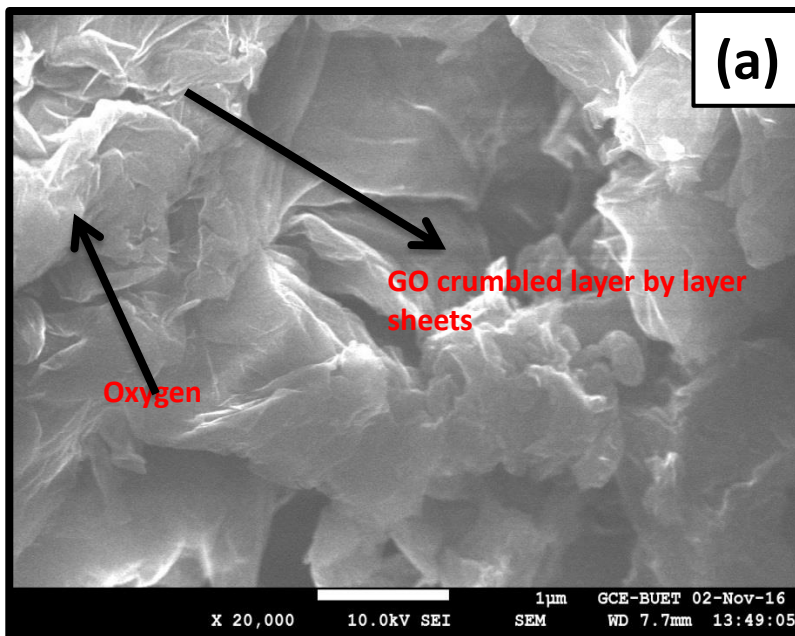
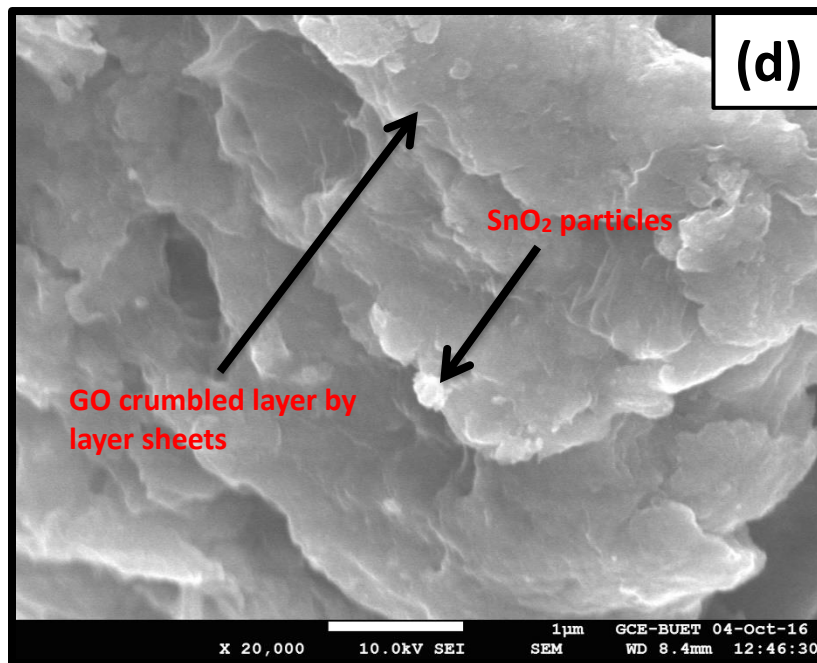
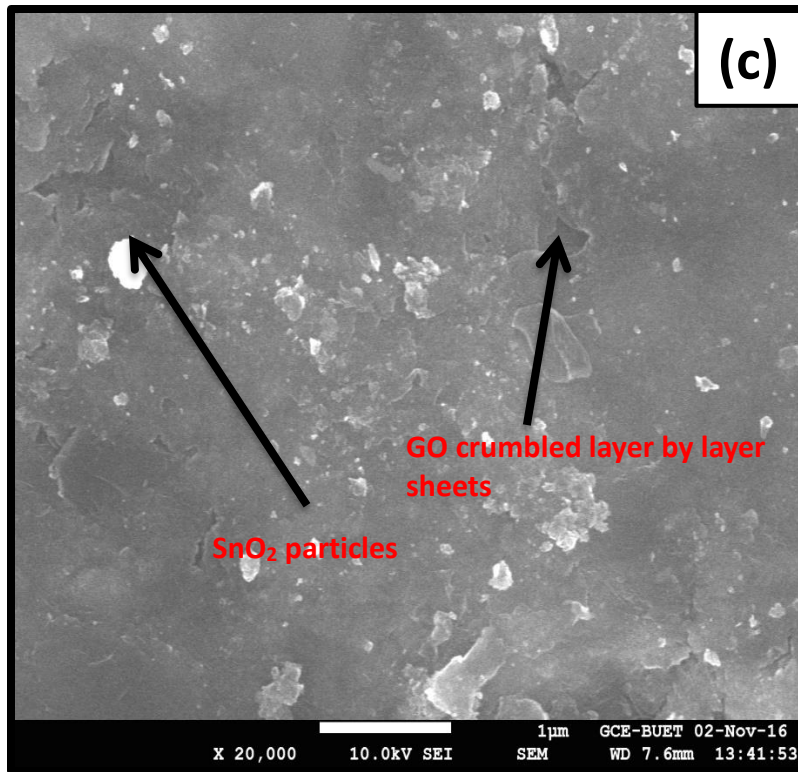


Fig. 1: XRD of Graphite, GO, SnO₂, GO-SnO₂ and rGO-SnO₂





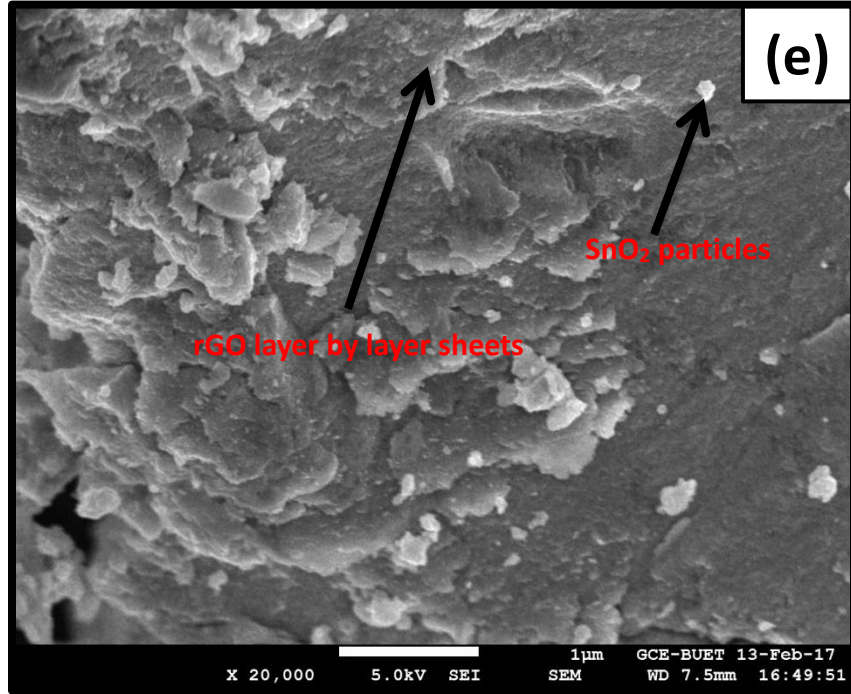
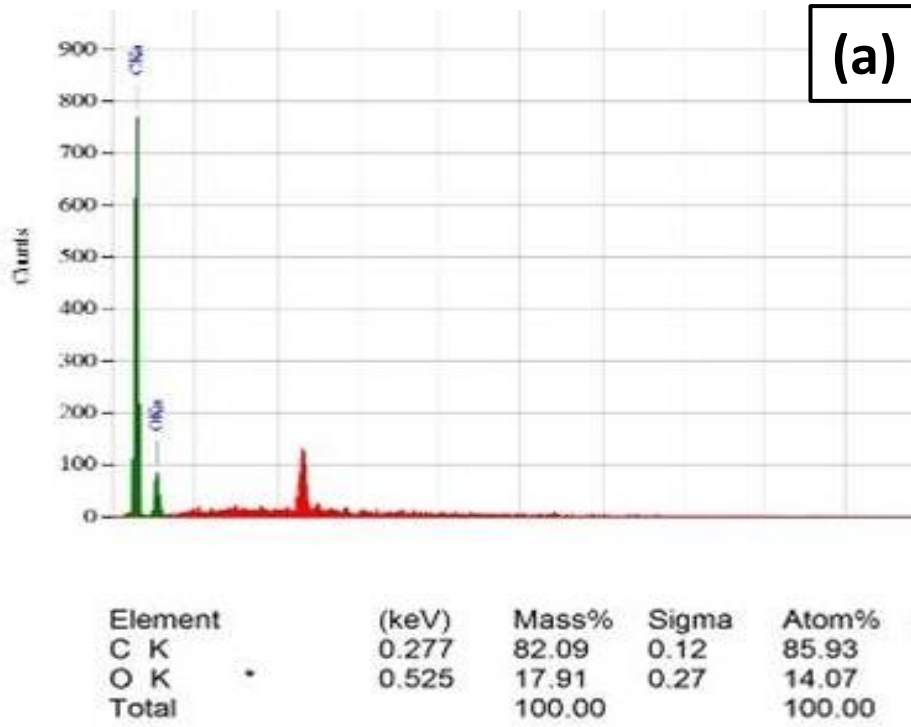
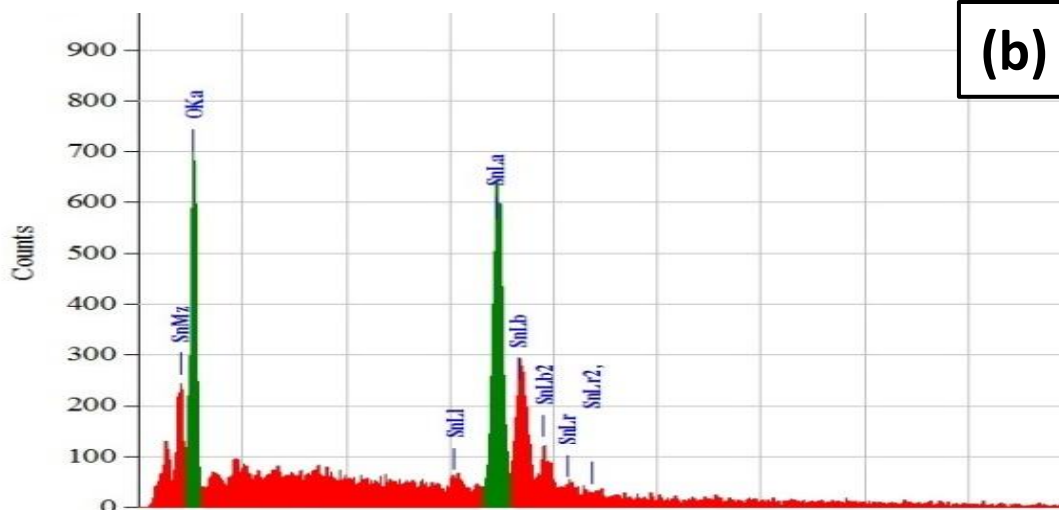


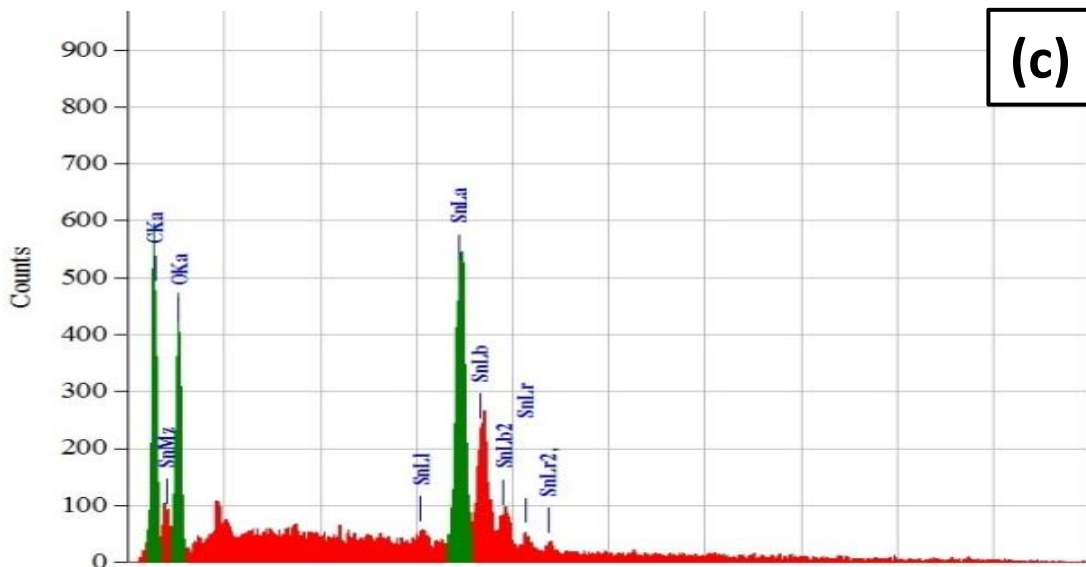
Fig. 2: SEM of (a) GO, (b) SnO₂, (c,d) GO-SnO₂ and (e) rGO-SnO₂





(b)

Element	(keV)	Mass%	Sigma	Atom%
O K	0.525	30.21	0.43	76.25
Sn L	3.442	69.79	0.94	23.75
Total		100.00		100.00



(c)

Element	(keV)	Mass%	Sigma	Atom%
C K *	0.277	15.05	0.03	41.42
O K	0.525	19.54	0.14	40.37
Sn L	3.442	65.40	0.54	18.21
Total		100.00		100.00

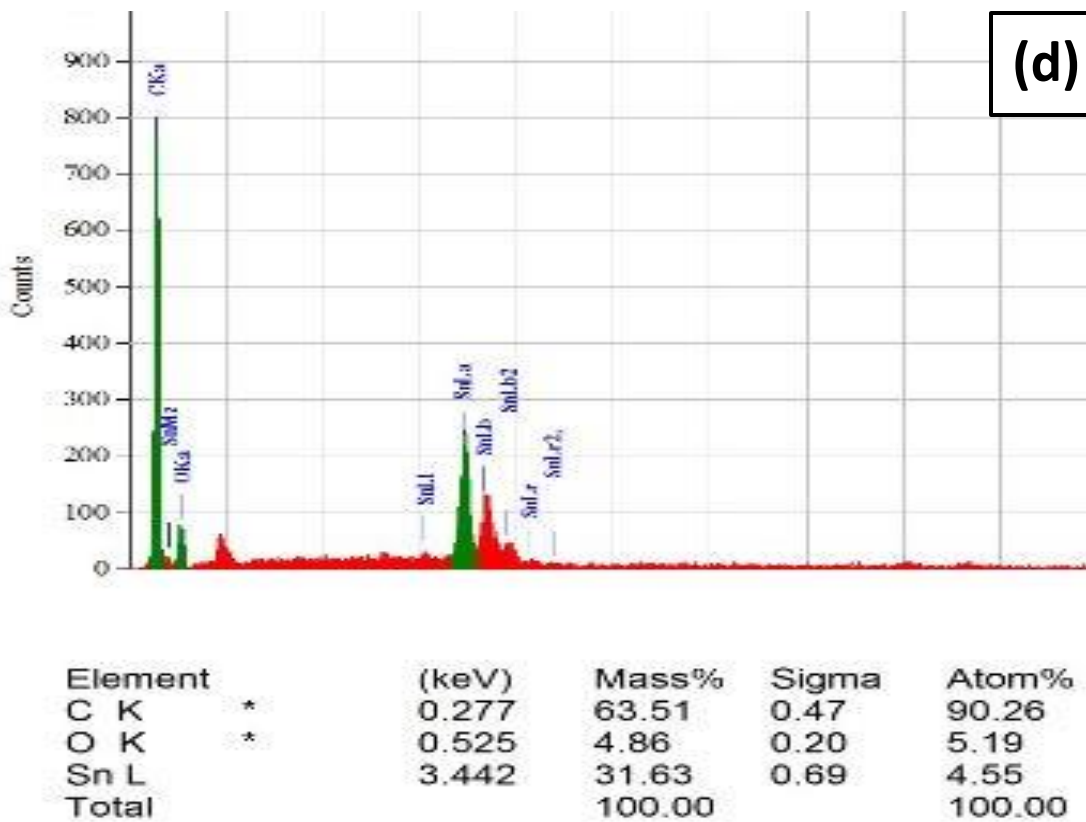


Fig. 3: EDX spectra of (a) GO, (b) SnO₂, (c) GO-SnO₂ and (d) rGO-SnO₂

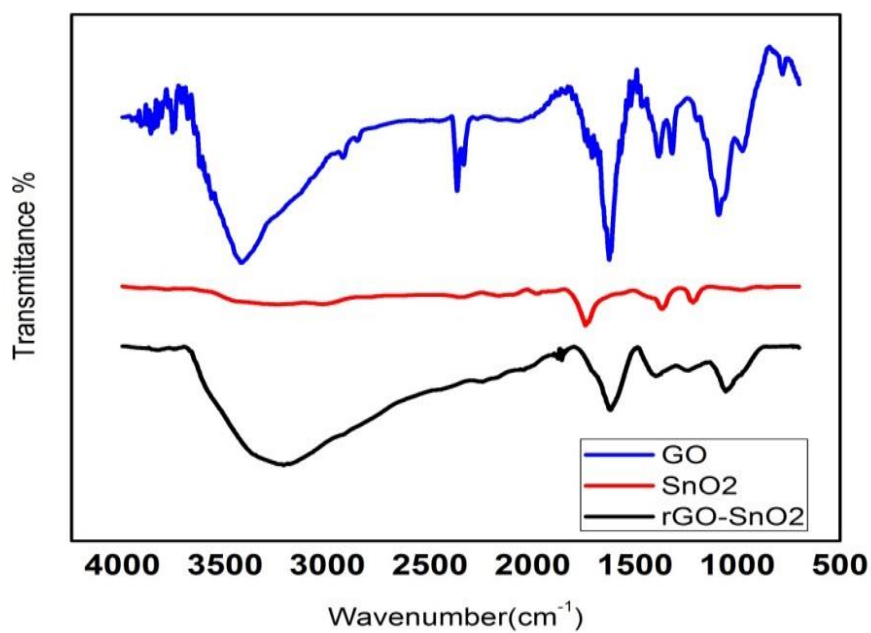
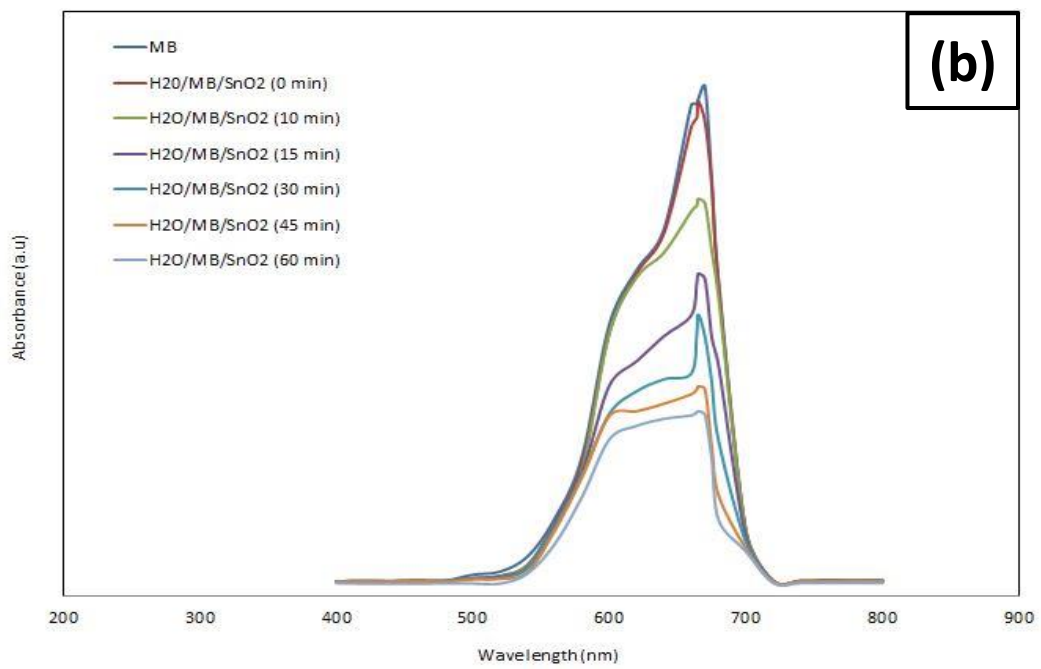
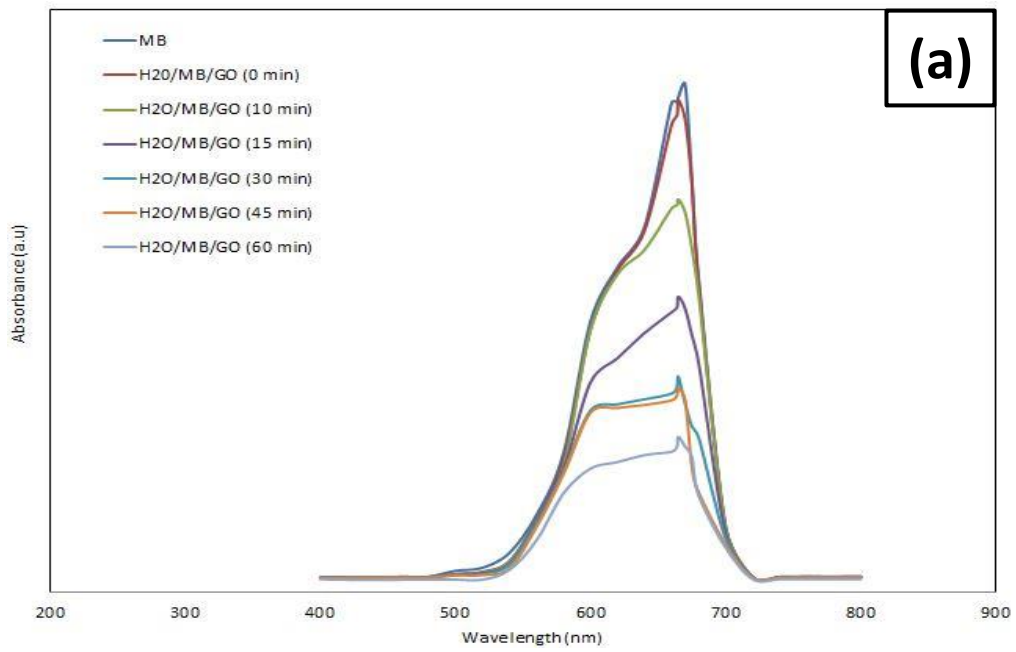
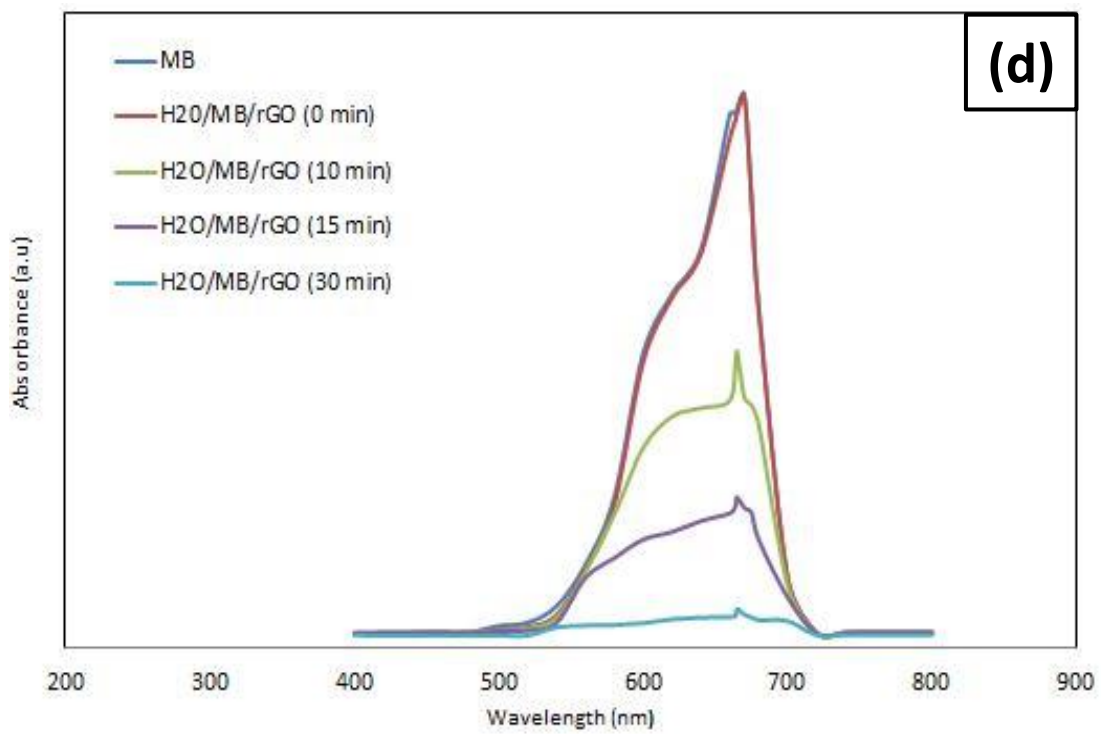
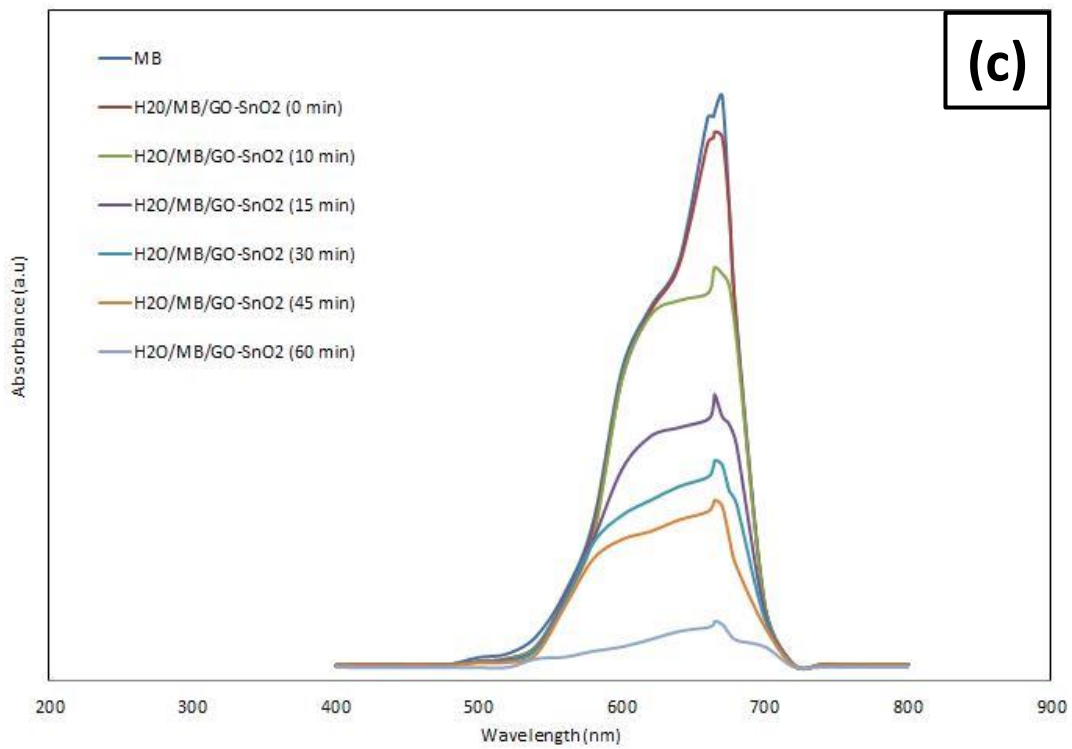


Fig. 4: FTIR curves of GO, SnO₂ and rGO-SnO₂





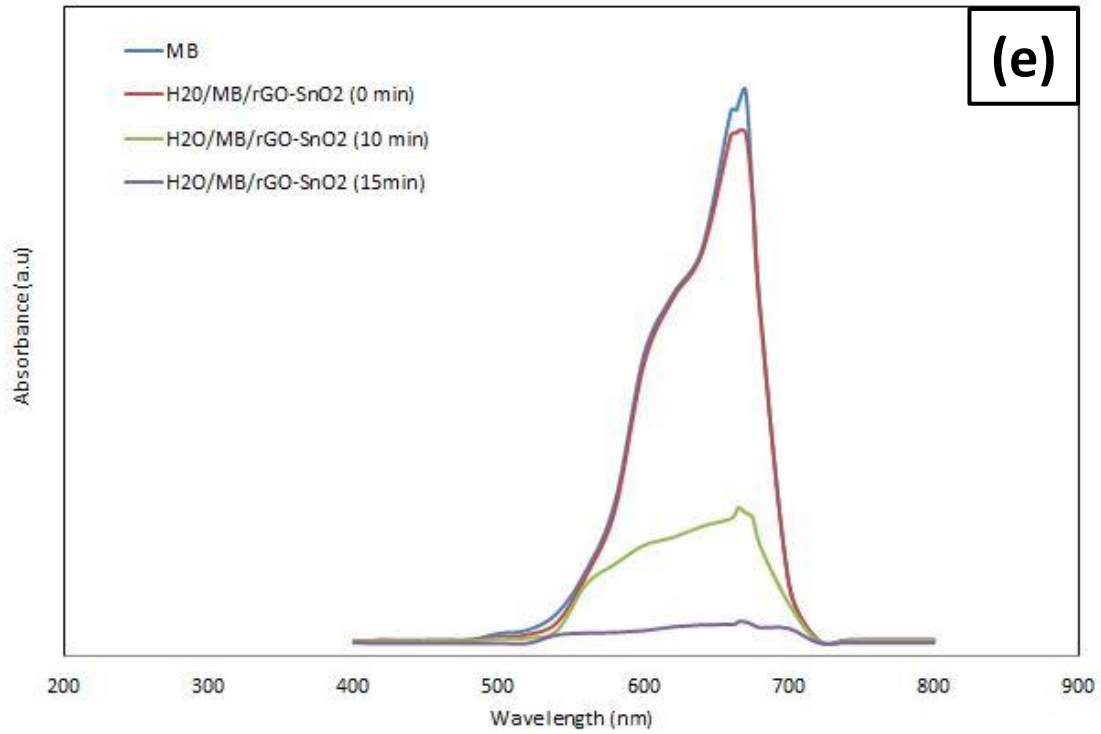


Fig. 5: Time-dependent absorption spectra of MB solution during natural sunlight irradiation in the presence (a) GO, (b) SnO₂, (c) GO-SnO₂, (d) rGO and (e) rGO-SnO₂

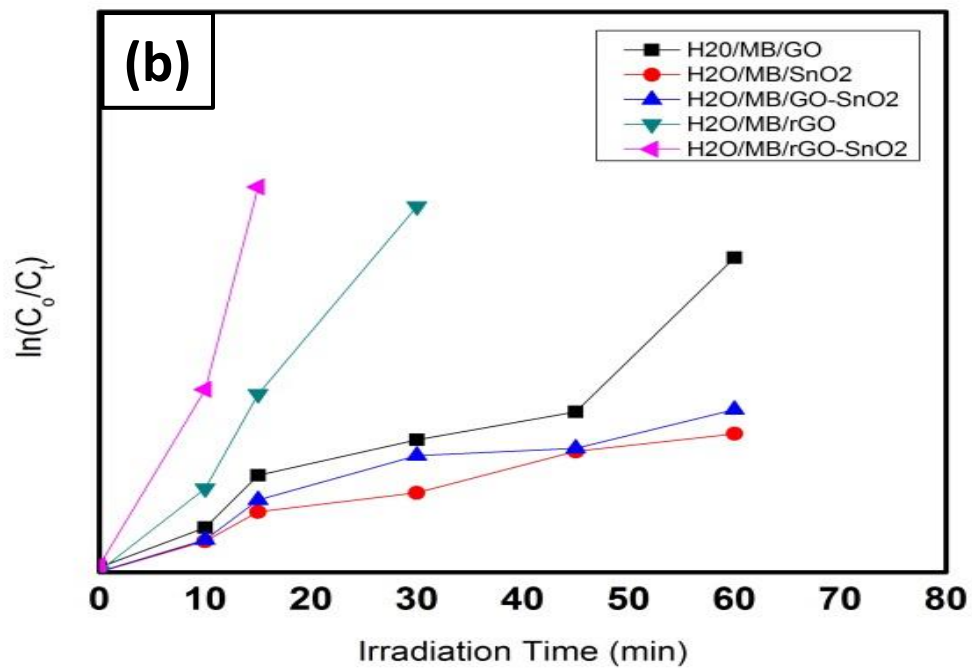
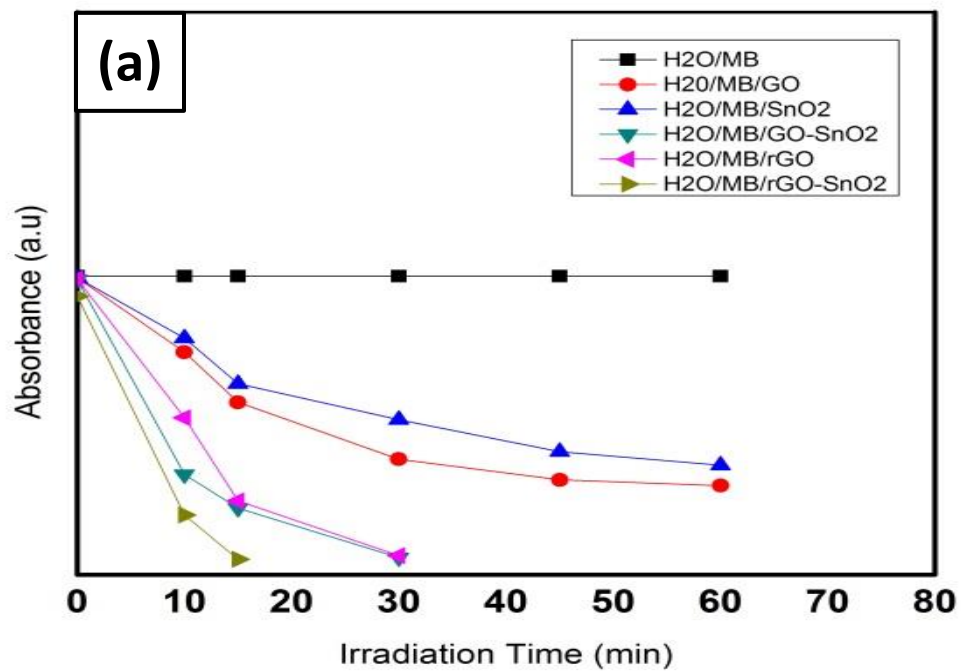
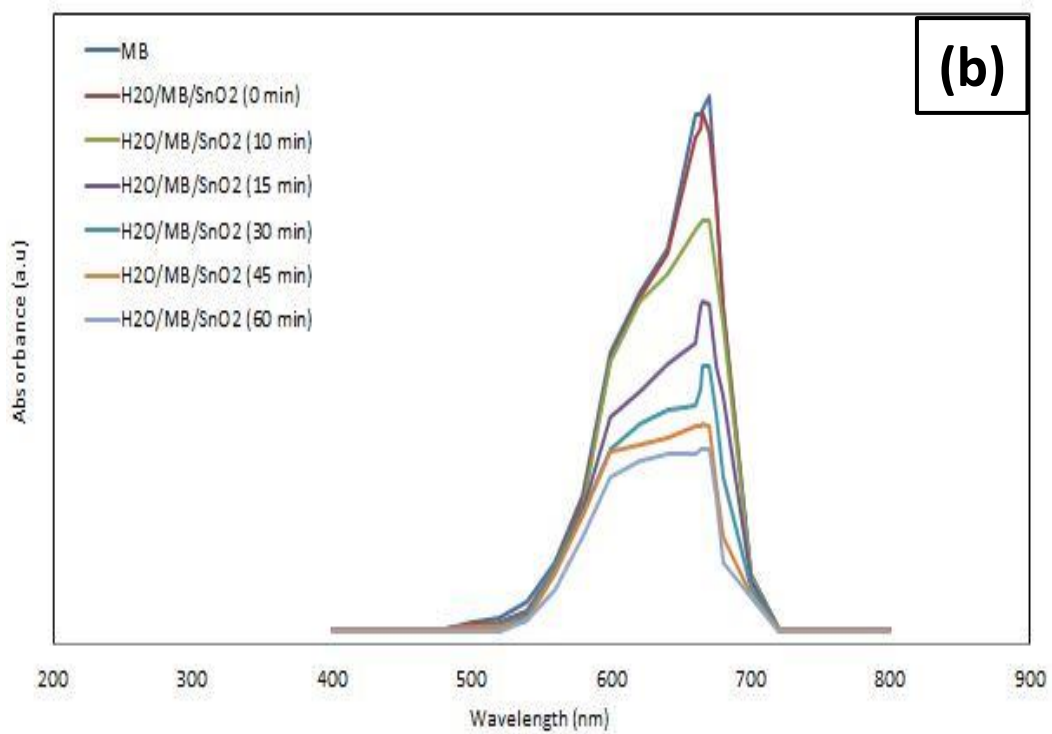
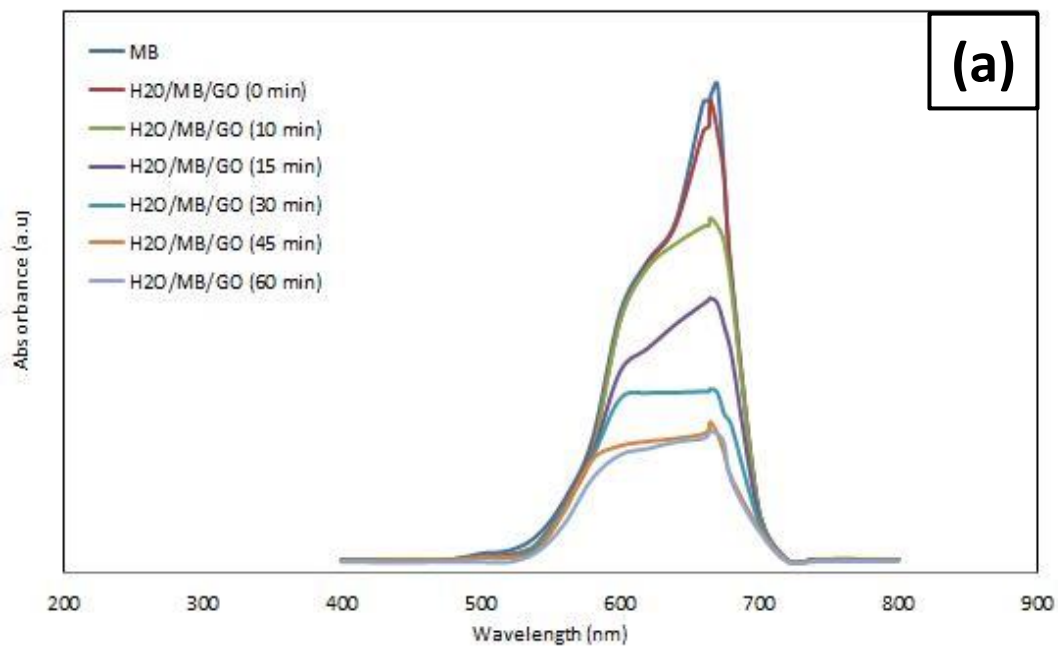
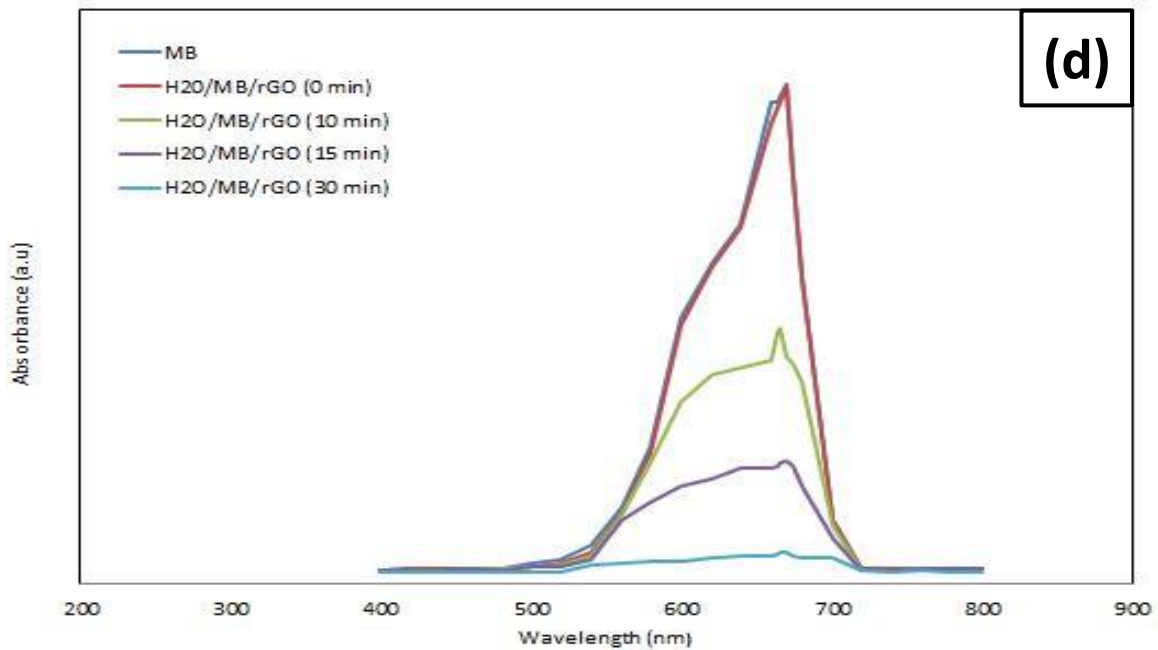
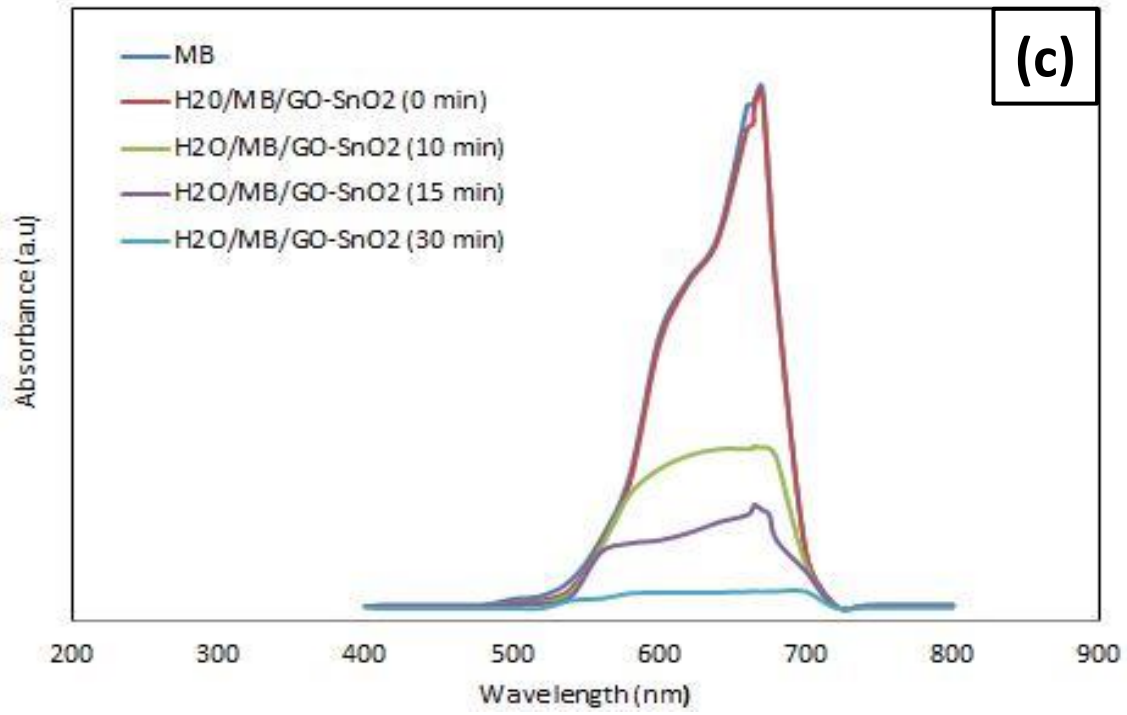


Fig. 6: (a) Absorbance versus Irradiation time curves for GO, SnO₂, GO-SnO₂, rGO and rGO-SnO₂ and (b) $\ln(C_0/C_t)$ versus Irradiation time curves illustrating MB photodegradation by GO, SnO₂, GO-SnO₂, rGO and rGO-SnO₂





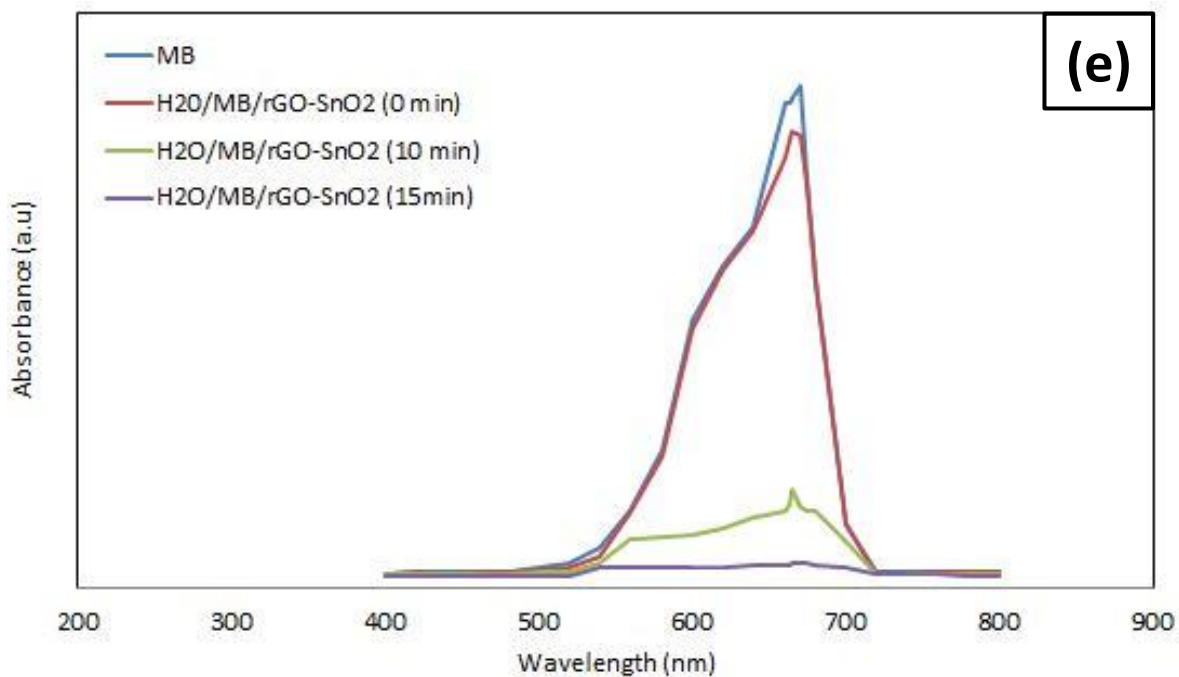
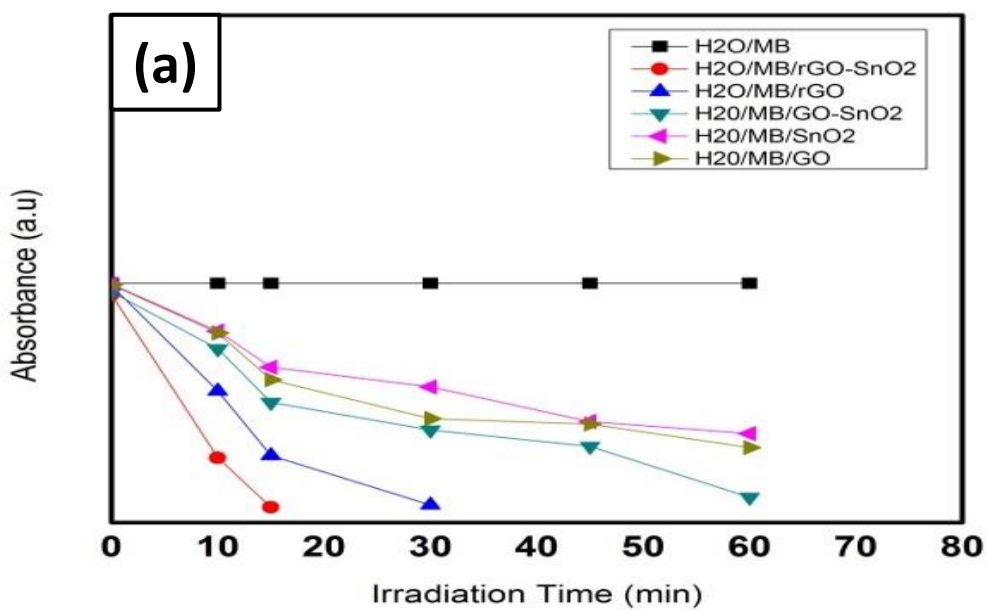


Fig. 7: Time-dependent absorption spectra of MB solution during UV light irradiation in the presence (a) GO, (b) SnO₂, (c) GO-SnO₂, (d) rGO and (e) rGO-SnO₂



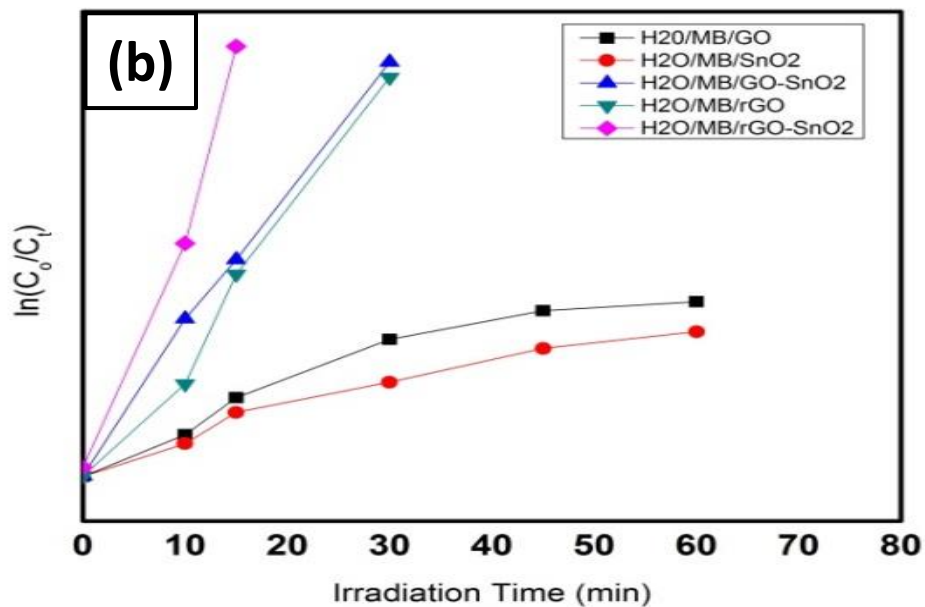
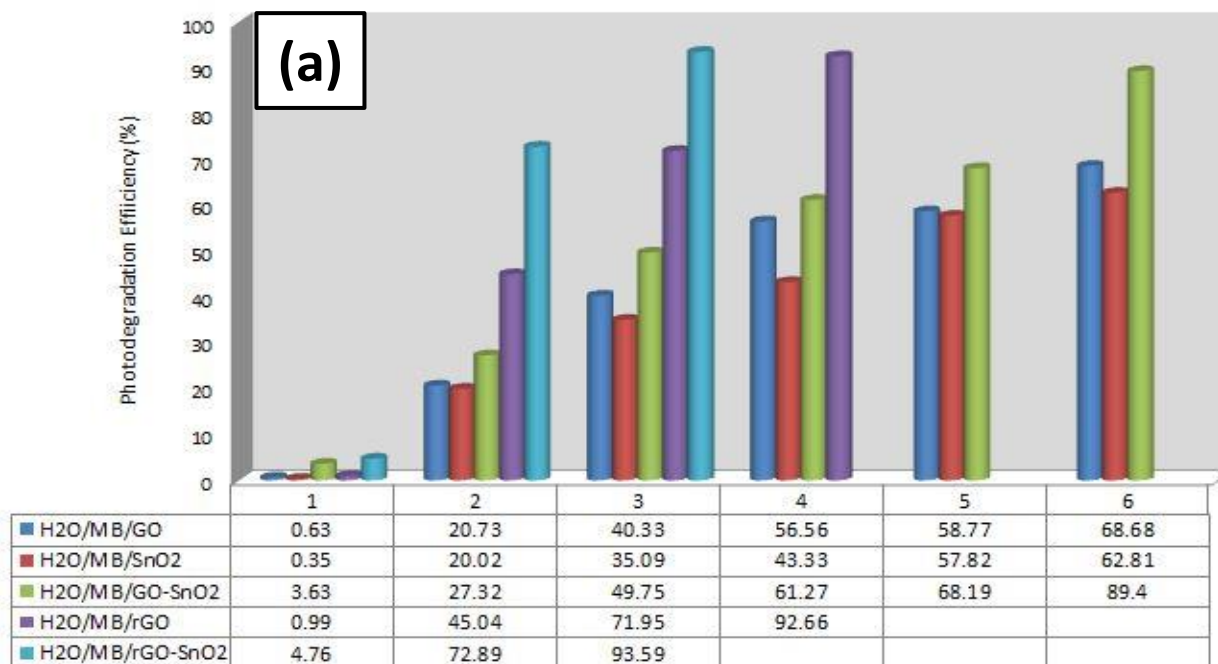


Fig. 8: (a) Absorbance versus Irradiation time curves for GO, SnO₂, GO-SnO₂, rGO and rGO-SnO₂ and (b) $\ln(C_0/C_t)$ versus UV light Irradiation time curves illustrating MB photo degradation by GO, SnO₂, GO-SnO₂, rGO and rGO-SnO₂



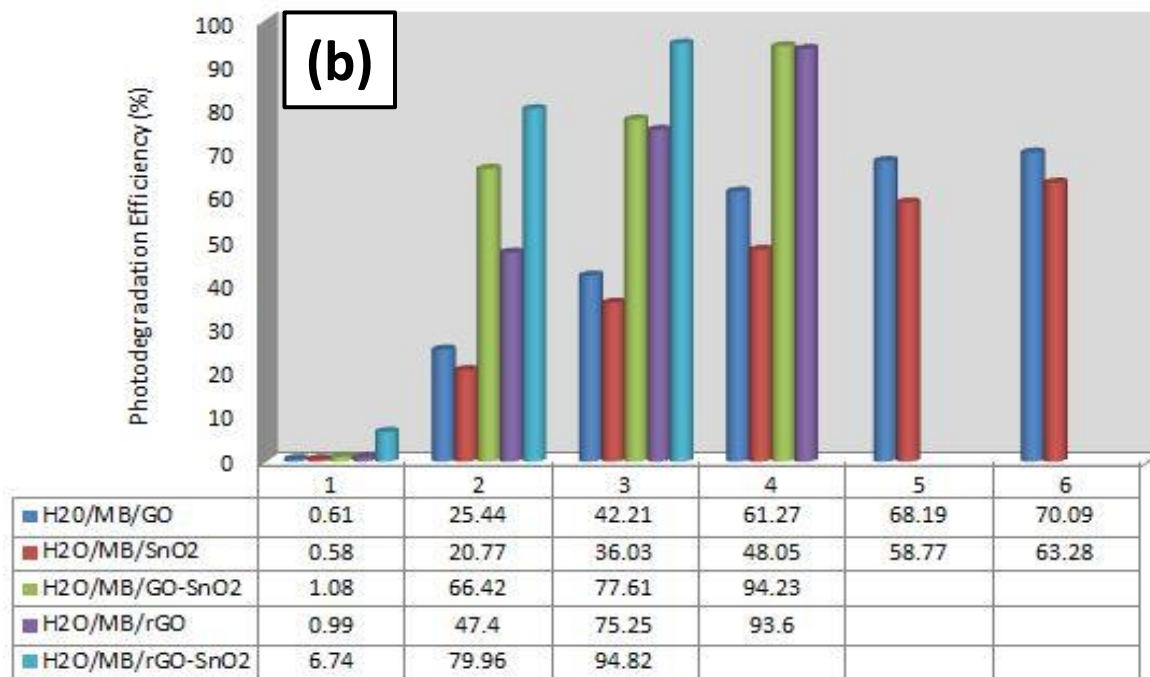
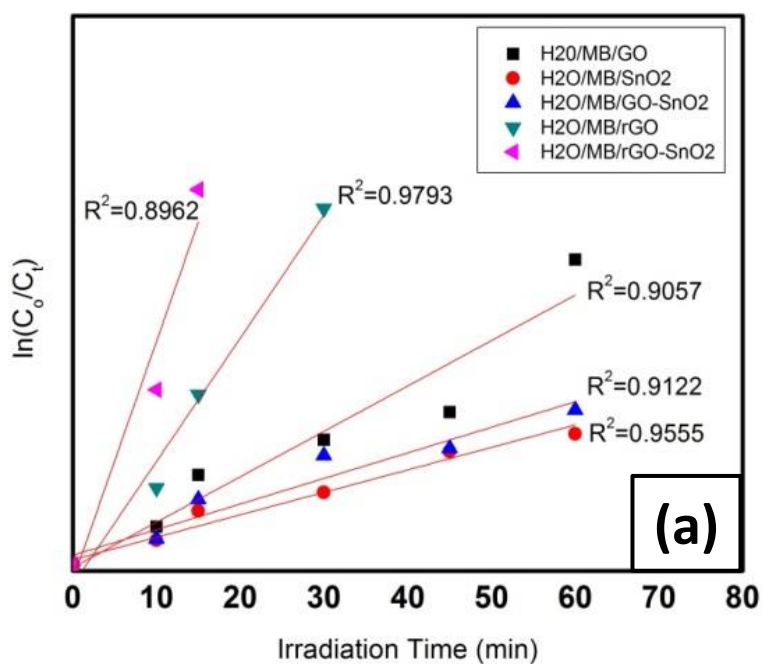


Fig. 9: Photodegradation Efficiency (%) under (a) Natural Sunlight and (b) UV light



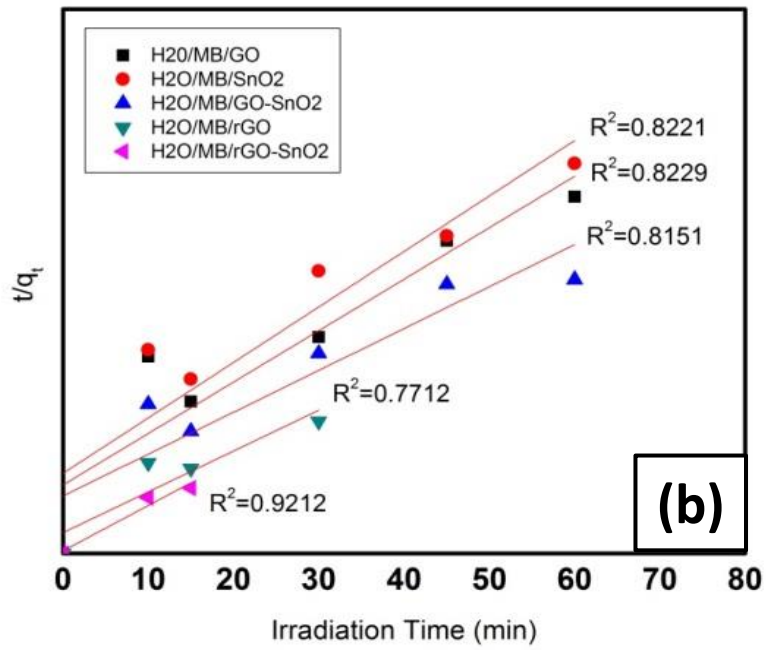
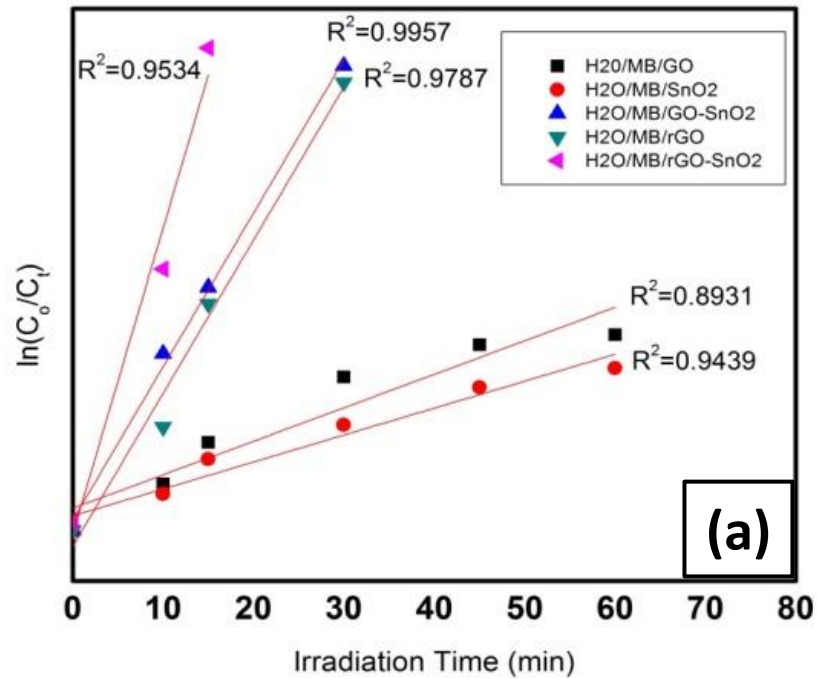


Fig. 10: The correlation coefficient (R^2) values for (a) pseudo-first order and (b) pseudo-second order under natural sunlight irradiation.



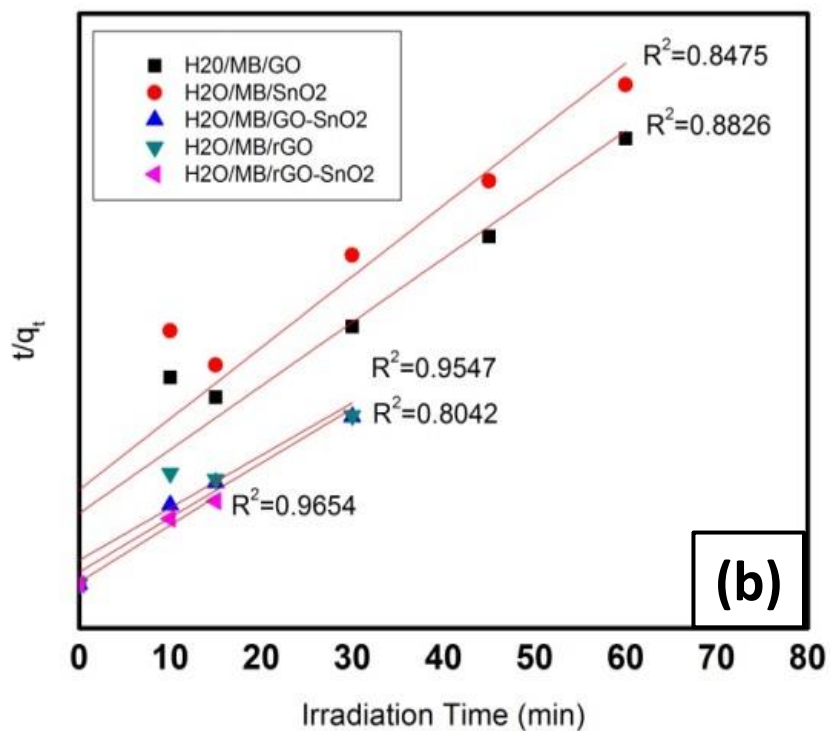


Fig. 11: The correlation coefficient (R^2) values for (a) pseudo-first order and (b) pseudo-second order under UV light irradiation.

TABLES

Table 1. Properties of Methylene Blue (MB).

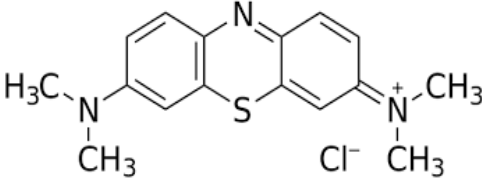
Properties	Cationic Azo Dye
Synonym name	Basic Blue 9
Molecular formula	C ₁₆ H ₁₈ ClN ₃ S
Molecular weight	319.851 g/mol
Absorbance wavelength(λ_{max})	664 nm
Molecular structure	

Table 2. The photocatalytic degradation of MB using several catalysts.

Authors/Year	Catalysts	Degradation efficiency (%)	Conditions	References
Soltani <i>et al.</i> 2014	BiFeO ₃	100% MB	Time: 80 min; Catalyst loading: 0.5 g/L ⁻¹ ; Irradiation: Natural Sunlight; pH 2.5	[5]
Dariani <i>et al.</i> 2016	TiO ₂	100% MB	Time: 2 hr; Catalyst loading: 0.5 g/L ⁻¹ ; Irradiation: UV light; pH 2.5	[6]

Table 3. Degradation efficiency and pseudo-first order rate constant for photocatalytic degradation of MB by GO, SnO₂, GO-SnO₂, rGO and rGO-SnO₂ under natural sunlight irradiation:

Samples	Concentration of MB (mM)	Degradation Efficiency (%)	R²	Rate constant (min⁻¹)
H ₂ O/MB/GO	0.05	68.68%	0.9057	0.0374
H ₂ O/MB/SnO ₂	0.05	62.81%	0.9555	0.0165
H ₂ O/MB/GO-SnO ₂	0.05	89.4%	0.9122	0.0193
H ₂ O/MB/rGO	0.05	92.66%	0.9793	0.0870
H ₂ O/MB/rGO-SnO ₂	0.05	93.59%	0.8962	0.1833

Table 4. Degradation efficiency and pseudo-second order rate constant for photocatalytic degradation of MB by GO, SnO₂, GO-SnO₂, rGO and rGO-SnO₂ under natural sunlight irradiation:

Samples	Concentration of MB (mM)	Degradation Efficiency (%)	R²	Rate constant (mM⁻¹min⁻¹)
H ₂ O/MB/GO	0.05	68.68%	0.8229	0.3641
H ₂ O/MB/SnO ₂	0.05	62.81%	0.8221	0.2816
H ₂ O/MB/GO-SnO ₂	0.05	89.4%	0.8151	1.4059
H ₂ O/MB/rGO	0.05	92.66%	0.7712	4.2079
H ₂ O/MB/rGO-SnO ₂	0.05	93.59%	0.9212	9.75

Table 5. Degradation efficiency and pseudo-first order rate constant for photocatalytic degradation of MB by GO, SnO₂, GO-SnO₂, rGO and rGO-SnO₂ under UV light irradiation:

Samples	Concentration of MB (mM)	Degradation Efficiency (%)	R²	Rate constant (min⁻¹)
H ₂ O/MB/GO	0.05	70.01%	0.8931	0.0201
H ₂ O/MB/SnO ₂	0.05	63.28%	0.9439	0.0167
H ₂ O/MB/GO-SnO ₂	0.05	94.23%	0.9957	0.0951
H ₂ O/MB/rGO	0.05	93.6%	0.9787	0.0916
H ₂ O/MB/rGO-SnO ₂	0.05	94.82%	0.9534	0.1974

Table 6. Degradation efficiency and pseudo-second order rate constant for photocatalytic degradation of MB by GO, SnO₂, GO-SnO₂, rGO and rGO-SnO₂ under UV light irradiation:

Samples	Concentration of MB (mM)	Degradation Efficiency (%)	R²	Rate constant (mM⁻¹min⁻¹)
H ₂ O/MB/GO	0.05	70.01%	0.8826	0.3904
H ₂ O/MB/SnO ₂	0.05	63.28%	0.8475	0.2872
H ₂ O/MB/GO-SnO ₂	0.05	94.23%	0.8042	5.4437
H ₂ O/MB/rGO	0.05	93.6%	0.9547	4.8750
H ₂ O/MB/rGO-SnO ₂	0.05	94.82%	0.9654	12.2033

GRAPHICAL ABSTRACT

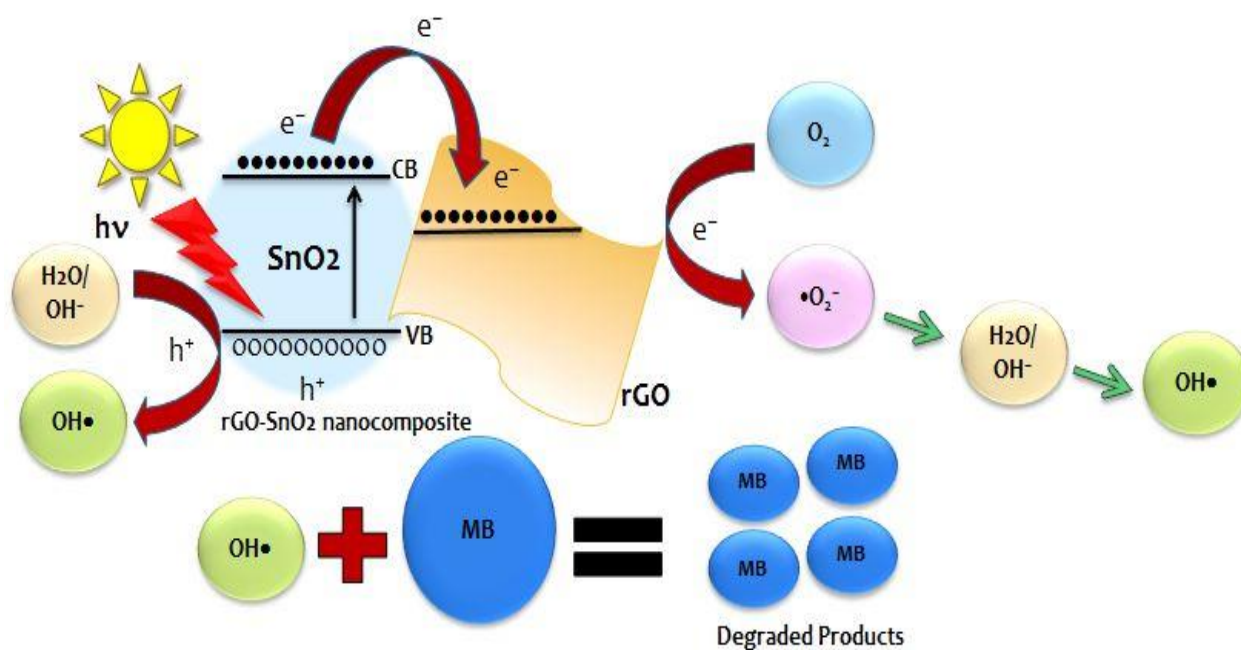


Fig. (A): Photodegradation of MB using rGO-SnO₂ nanocomposite under sunlight irradiation

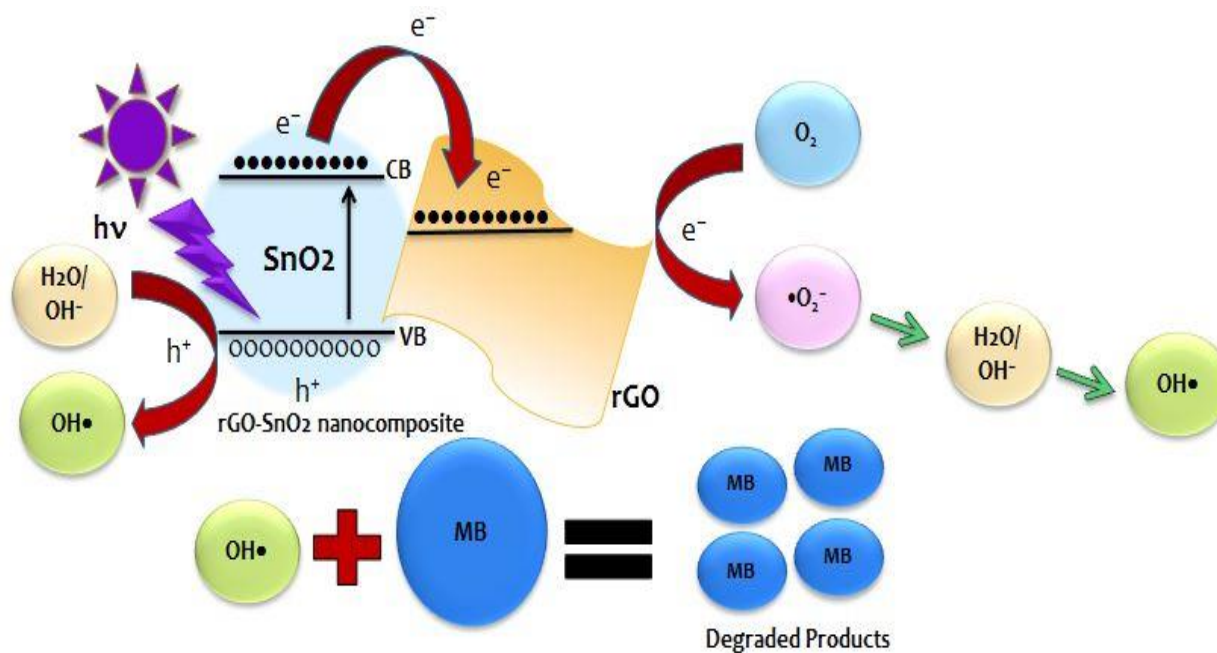


Fig. (B): Photodegradation of MB using rGO-SnO₂ nanocomposite under UV light irradiation